Project Kestrel

The Millennium Falcons Design Team

Robbie Sorrentino, Caleb Mallicoat, Andrew Kraemer,
Ryan Hughes, Alfredo Basile, Ben Hamer, Riley Assaid

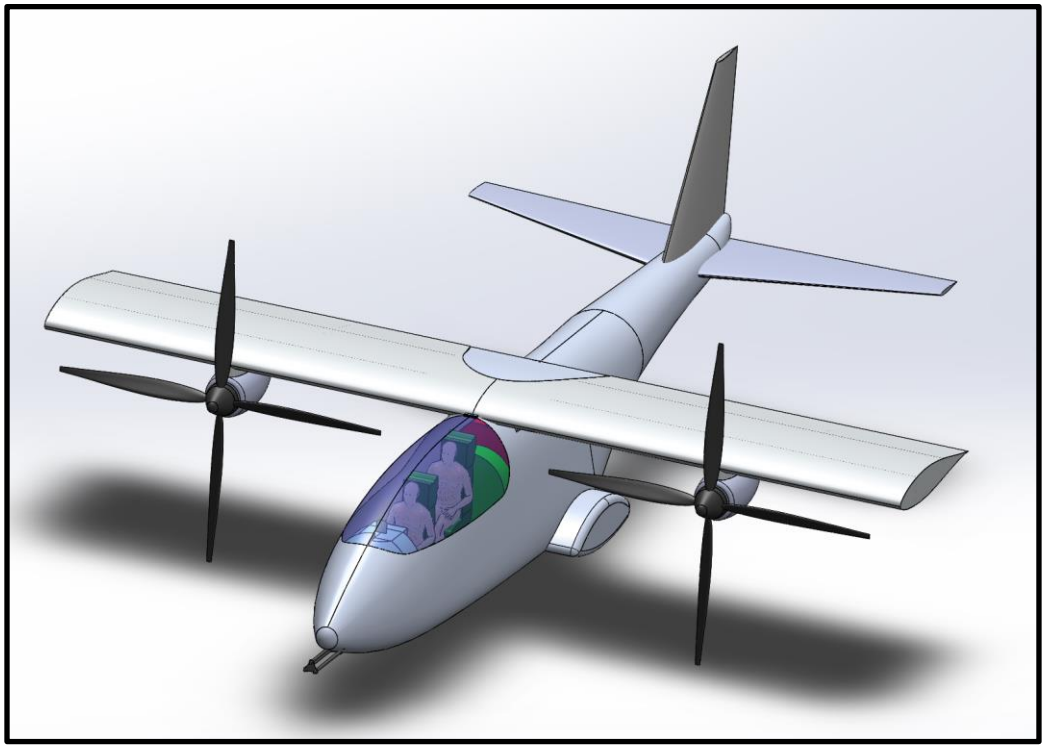

AIAA 2020-2021 Undergraduate Aircraft Design RFP
Austere Field Light Attack Aircraft

Department of Mechanical and Aerospace Engineering

Faculty Advisor: Dr. Jesse Quinlan

Date of Submission: May 13, 2021

The Millennium Falcons Design Team

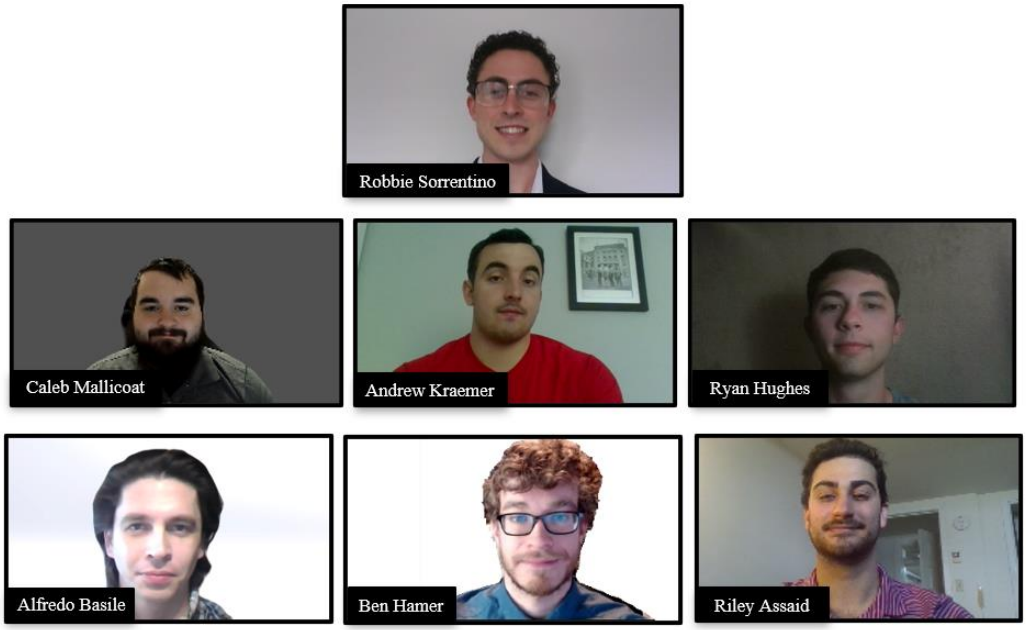

Team Member	Signature	AIAA Member Number	Role
Robbie Sorrentino		1180395	Team Leader Mission Performance
Caleb Mallicoat		1180095	Propulsion
Andrew Kraemer		1180549	Propulsion
Ryan Hughes		1241354	Cost
Alfredo Basile		1180268	Structures
Ben Hamer		1180297	Stability & Control
Riley Assaid		1180217	Aerodynamics
Dr. Jesse Quinlan		306245	Faculty Advisor

Contents

I. Acknowledgements

The team would like to thank Dr. Jesse Quinlan and Mr. David Eames for their guidance on the design of the Kestrel. Your continuing support is very much appreciated and the project would not be what it is without your contributions. The team would also like to acknowledge and thank Sander Abraham, a fellow classmate, for assistance with scripting the process of formatting GasTurb output with Python for use in mission analysis.

II. List of Figures

III. List of Tables

IV. Abbreviations

AGM = Air-To-Ground Missile

AOA = Angle of Attack

CAS = Close Air Support

CBR = California Bearing Ratio

C_g = Center-of-Gravity

C_L = Coefficient of Lift

DF = Direction Finding

DOC = Direct Operating Cost

DOD = Department of Defense

EAP = Electric Aircraft Propulsion

EDET = Empirical Drag Estimation Technique

EIS = Entry Into Service

FFAR = Folding Fin Aerial Rocket

FLIR = Forward-Looking Infrared

FLOPS = Flight Optimization System

GE = General Electric

HUD = Heads-Up Display

IFF = Identification Friend or Foe

ILS = Instrument Landing System

IRMA = Interactive Reconfigurable Matrix of Alternatives

ISR = Intelligence, Surveillance, and Reconnaissance

JSSG = Joint Service Specification Guide

KEAS = Knots Equivalent Airspeed

LAAR = Light Attack/Armed Reconnaissance

LAS = Light Air Support

LCC = Life-Cycle Cost

LFL = Landing Field Length

MAC = Mean Aerodynamic Chord

MDAO = Multidisciplinary Design Analysis and Optimization

MIT = Massachusetts Institute of Technology

OEW = Operating Empty Weight

RCS = Radar Cross Section

RFP = Request for Proposal

SFC = Specific Fuel Consumption

STOL = Short Takeoff and Landing

T/W = Thrust Loading

TACAN = Tactical Air Navigation System

TOFL = Take-Off Field Length

TOGW = Takeoff Gross Weight

TRL = Technology Readiness Level

UHF = Ultra High Frequency

VSTOL = Vertical and/or Short Takeoff and Landing

VOR = Very High Frequency Omni-Directional Range

V_{stall} = Stall Velocity

VTOL = Vertical Takeoff and Landing

W/S = Wing Loading

V. Executive Summary

This report documents the preliminary design of an austere field light attack aircraft as called for in the AIAA 2021 Undergraduate Design Competition Request for Proposal (RFP) [1]. This class of aircraft can be defined as any aircraft that is lightweight, carries a payload capable of providing close air support (CAS), provides intelligence, surveillance, and reconnaissance (ISR), and is capable of deploying and returning to an austere airfield. An austere airfield is defined by the Department of Defense (DOD) as any small airfield lacking one or more of the following: taxiway systems, ramp space, security, materials handling equipment, aircraft servicing, maintenance, navigation aids, weather observing sensors, and communications [2].

The primary mission of CAS and ISR is already filled by many platforms, however, the design requirements of cost, survivability, and time on station seem to be the driving force for a light, rugged and versatile aircraft. The role of overcoming austere airfields, as an attack platform, has primarily been filled by rotors such as the AH-1 Cobra and the AH-64 Apache. These helicopters however are limited by their speed, range, maneuverability, flight ceiling, and large maintenance cost relative to fixed wing aircraft. Thus, the RFP calls for an aircraft that is capable of operating from short, austere fields near the front lines providing CAS to ground forces within short notice. Most importantly, this aircraft must be affordable and able to complete missions currently only feasible with attack helicopters. The aircraft must be able to take off and land in 4000 ft over a 50 ft obstacle when operating from austere fields. It must house two crew each with zero-zero ejection seats and must also hold a payload of 3000 lbs of armament. It must have a service life of 15,000 hours over 25 years and a service ceiling of 30,000 ft while being certifiable for military standard airworthiness according to MIL-STD-516C.

The Millennium Falcons present the Kestrel, a tiltwing light attack aircraft. The Kestrel has a 35 ft wingspan and is 40 ft long. It features a conventional tail and two wing-mounted General Electric (GE) T700 turboshaft engines. The Kestrel can hold 3000 lbs of armament internal to its fuselage. It can take off in 709 ft and land in 496 ft on austere fields up to 6,000 ft in altitude. The Kestrel has a service life that exceeds 15,000 hours over 25 years and has a service ceiling of 38,800 ft. The takeoff gross weight (TOGW) and operating empty weight (OEW) of the Kestrel are 14,170 lbs and 9157 lbs, respectively. The average acquisition, life cycle cost (LCC), and direct operating cost (DOC) for the procurement of 150 aircraft with an entry into service (EIS) of 2025, are $20.42 million, $3870 per flight hour, and $11.97 billion, respectively. The Kestrel meets all of the design requirements and

objectives set forth by the RFP and offers a compelling and affordable alternative to conventional light attack aircraft.

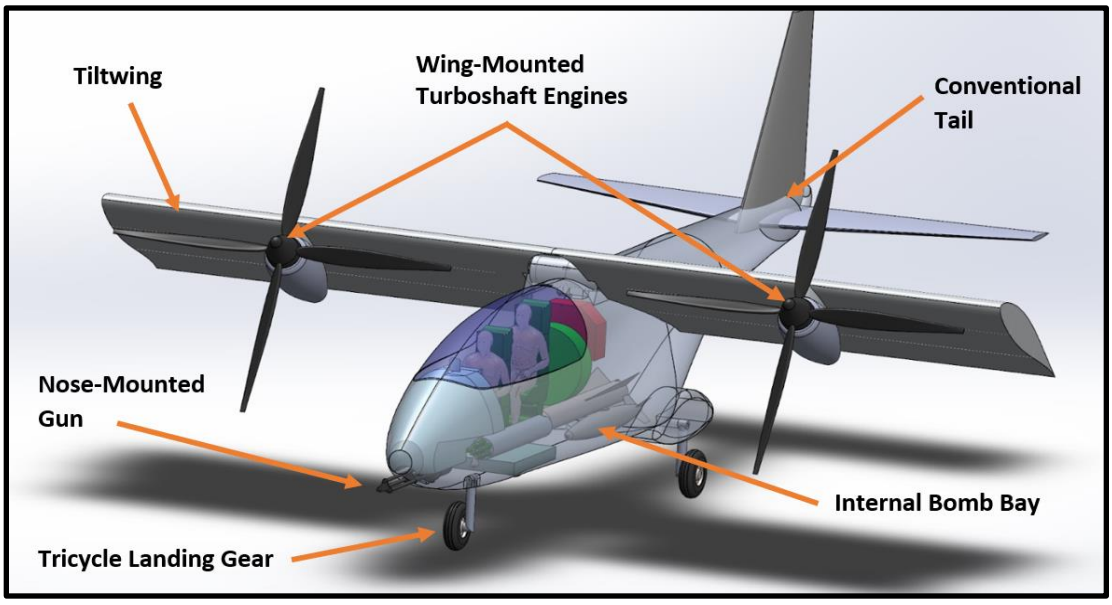

Figure 1: Vehicle Overview

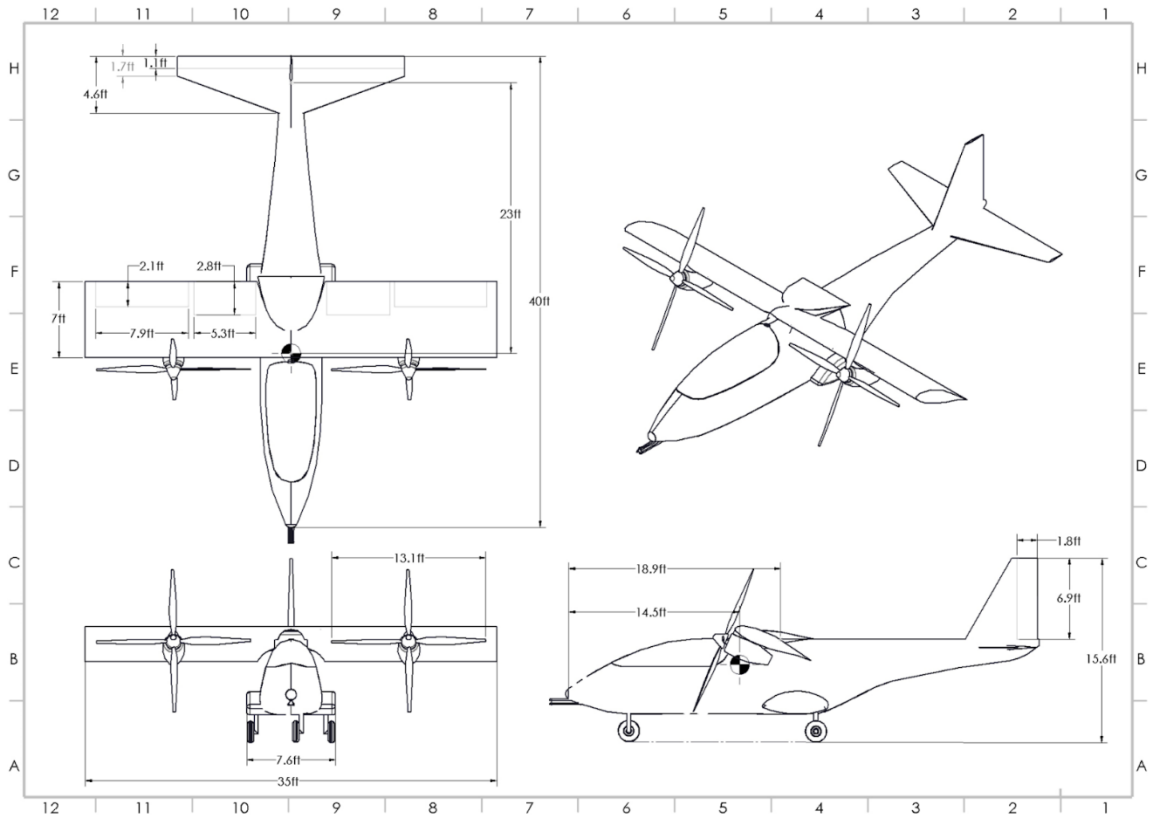

Figure 2: Dimensioned 3-View

Table 1: Key Performance Parameters

Gross Weight	14,170 lbs
Operating Empty Weight	9157 lbs
Block Fuel Burn	1795 lbs
Block Time	5.01 hours
Wing Area	245 ft^2
Maximum Lift-to-Drag Ratio	12.9
Top Speed	394 mph
Specific Fuel Consumption	0.43 lbm/hp/hr
Acquisition Cost	$20.42 M
Operating Cost	$3870/hr
Life-Cycle Cost	$11.97 B

VI. Requirements Analysis

VI.A RFP Requirements

The general requirements set by the RFP are listed below in Table 2. The austere field performance, payload, and service ceiling requirements have the greatest impact on the design of a suitable aircraft. Affordability and helicopter-like utility were added as derived objectives because of the RFP's description of low cost and helicopter operations as desirable.

Table 2: Requirements: [R] = Mandatory Requirement [O] = Objective or Goal [DO] = Derived Objective

Item	Criteria
Austere Field Performance [R]	TOFL and LFL ≤ 4000 ft over 50 ft obstacle
Survivability [O]	Armor, infrared signature, countermeasure, etc.
Payload [R]	3000 lbs of armament
Weapon Provisions [O]	Rail-launched missiles, rockets, 500 lb bombs
Integrated Gun [R]	Used for ground targets
Service Life [R]	15,000 hours over 25 years
Service Ceiling [R]	≥ 30,000 ft
Crew [R]	Two, both with zero-zero ejection seats
Affordability [DO]	Considerations for reduced cost
Helicopter-Like Utility [DO]	Capable of completing VTOL missions

The integrated gun was assumed to be included in the 3000 lbs of armament per the payload requirement. The weight of each crew member and their equipment was assumed to be 200 lbs. Additionally, the crew were assumed to be 6 feet tall. The objectives of survivability and weapon provisions were tradable. All other requirements are mandatory and must be satisfied by the design. When making technology decisions, an entry into service of 2025 was assumed. Critical technologies needed to be a technology readiness level (TRL) 8 or above. TRL 8 technology means the actual system has been completed and "flight qualified" through test and demonstration [3]. All critical technologies selected for the design of the Kestrel, such as the actuator system, engine, materials, etc., have been used on previous or current aircraft and meet the TRL 8 requirement.

VI.B Comparator Aircraft Identification

The two aircraft closest to meeting all of the requirements specified in the RFP are the A-29 Super Tucano and the AT-6 Wolverine. The CL-84 Dynavert was also added as a comparator due to its similarity in design as a tiltwing aircraft. Table 3 summarizes that these comparator aircraft already meet the major requirements outlined in the RFP [4-11].

Table 3: Comparator Aircraft Compliance Matrix

Item	Criteria	A-29	AT-6	CL-84	Kestrel
Austere Field Performance [R]	TOFL and LFL ≤ 4000 ft over 50 ft obstacle	Yes, TOFL = 2,953 ft LFL = 2,821 ft	Yes, TOFL and LFL ~ A-29	Yes, TOFL and LFL ~ 500 ft	Yes, TOFL = 709 ft LFL = 496 ft
Survivability [O]	Armor, infrared signature, countermeasures, etc.	Yes	Yes	Yes	Yes
Payload [R]	3000 lbs of armament	Yes, 3300 lbs	Yes, 4110 lbs	Yes, 4035 lbs	Yes, 3000 lbs
Weapon Provisions [O]	Rail-launched missiles, rockets, 500 (lb) bombs	Yes	Yes	Yes	Yes
Integrated Gun [R]	Used for ground targets	Yes	Yes	Yes	Yes
Service Life [R]	15,000 hours over 25 years	Unknown	Unknown	Unknown	Yes
Service Ceiling [R]	≥ 30,000 ft	Yes, 35,000 ft	Yes, 31,000 ft	Unknown	Yes, 38,800 ft
Crew [R]	Two, both with zero-zero ejection seats	Yes	Yes	Yes	Yes
Affordability [DO]	Considerations for reduced cost	Yes	Yes	Yes	Yes
Helicopter-Like Utility [DO]	Capable of completing VTOL missions	No	No	Yes	Yes

Considering that both the A-29 and AT-6 aircraft are on the market and already meet the mandatory performance requirements in the RFP, they served as existing baselines from which to improve on. The door is open for a new and unique light attack aircraft that offers greater versatility and mission flexibility.

VI.C Certification

The certification requirements that are critical to the design of the Kestrel can be found in MIL-HDBK-516C and the DOD's Joint Service Specification Guides (JSSG), such as JSSG-2001 Air Vehicle and JSSG-2006 Aircraft Structures [12-14]. The key definitions in these documents influence the analysis of the design in meeting service ceiling and service life requirements. Service ceiling is defined as the altitude at which the maximum steady state rate-of-climb potential is 100 feet per minute for a specified configuration, weight, speed and power setting. The aircraft must also meet a factor of safety of 1.5 or higher when experiencing the design limit loads of -1 and 4g during maneuvering. These design limits set the bounds for the flight envelope of the Kestrel. The pilot must also have a minimum over-nose viewing angle of 11-15 degrees.

VI.D Concept of Operations

Figures 3 and 4 show the design and ferry mission profiles as specified in the RFP, respectively.

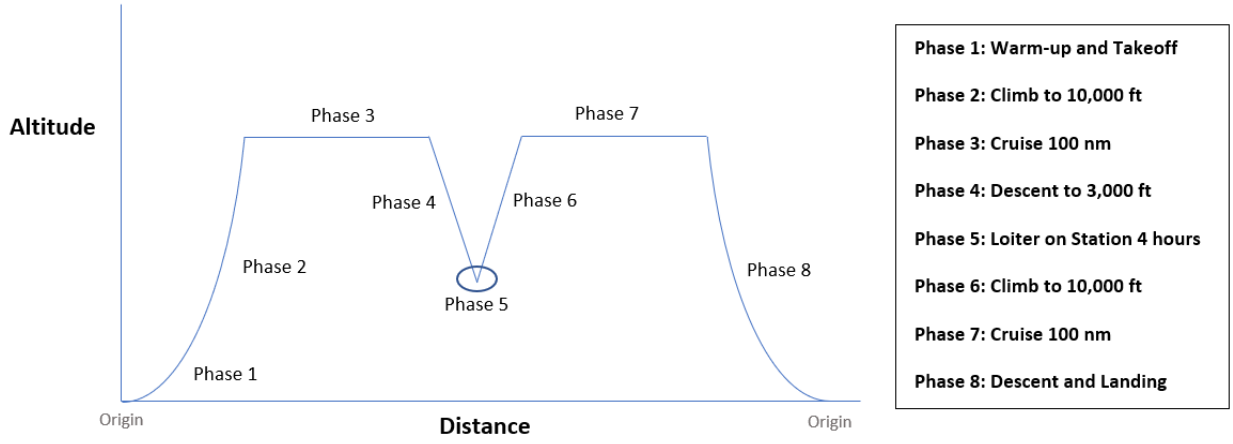

Figure 3: Design Mission Profile

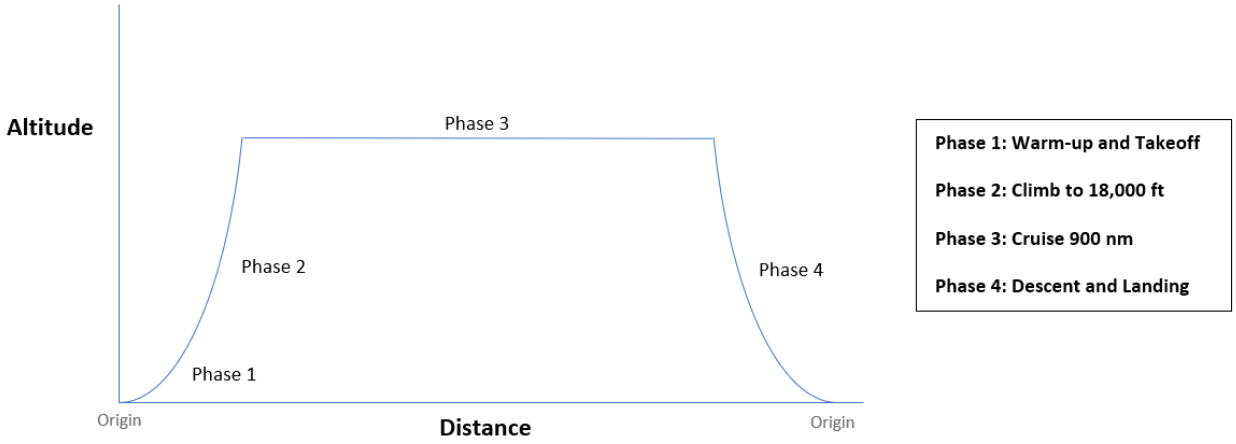

Figure 4: Ferry Mission Profile

The aircraft begins by warming up and taxiing for 5 minutes. It then must take off from an austere field in 4000 ft or less over a 50 ft obstacle. For the design mission, the aircraft must climb with range credit to at least 10,000 ft and then cruise 100 nm. The aircraft must then descend with no range credit to 3000 ft within 20 minutes of the initial climb. It was determined that the aircraft must cruise at a minimum of 0.47 Mach to achieve this result. The speed necessary to travel 100 nm in 20 minutes was found to be 345 mph. The minimum cruise speed was then calculated using the speed of sound at 10,000 ft of 734.5 mph. After descending to 3000 ft, the aircraft must loiter on station for 4 hours with no stores drops. It will then climb up to 10,000 ft and cruise back 100 nm before descending and landing with a taxi and shutdown time of 5 minutes. The ferry mission involves the same warm-up, takeoff, landing, and shutdown as the design mission. The ferry mission however involves only one climb, cruise, and descent segment. The aircraft must cruise 900 nm and can do so at best range speed. The key difference between the design and ferry missions is that the aircraft must carry the full payload requirement, 3000 lbs, for the design mission and only 60% of the payload requirement, 1800 lbs, for the ferry mission. Both missions require reserve fuel sufficient for climb to 3000 ft and loiter for 45 minutes.

VII. Configuration

VII.A Design Morphology

In order to rigorously explore potential configurations with high likelihood of meeting the design requirements, a coarse version of the Interactive Reconfigurable Matrix of Alternatives (IRMA) process was used to perform a concept down-select as a team. First, each individual member of the team proposed an initial light attack aircraft configuration by designing a model in OpenVSP, NASA's parametric aircraft geometry tool [15]. Next, a list of functional attributes was formed by establishing a complete taxonomy of the light attack aircraft. A morphological matrix of alternatives was then developed by identifying all the various features of the proposed concepts as shown in Table 4.

Table 4: Morphological Matrix

Functional Attributes		**Alternatives for Each Attribute**		
Fuselage	*Payload*	Wing hardpoints	Fuselage Hardpoints	Internal Bomb Bay
	Gun Armament	Centerline Cannon	Centerline MG(s)	Wing Mounted MGs
Wing	*Location*	Low	Mid	High
	Sweep	None	Slight	
	Dihedral	None	Slight	
	Taper	None	Slight	
	Wing Tilt	Fixed Level	Slight Fixed Tilt	Variable Tilt
S&C	*Pitch Effecter*	Conventional horizontal tail	V-tail	
	Yaw Effecter	Conventional vertical tail	Dual Vertical Stabilizer	
	Roll Effector	Conventional ailerons		
Propulsor Integration	*Location*	Nose Mounted	Wing Mounted	
	Type	Turboprop/Turboshaft	Hybrid Electric	
	Number	1	2	
	Fuel	Liquid	Liquid & Batteries	

After thorough analysis of the RFP, metrics of interest were determined to be takeoff and landing performance, survivability and maneuverability, payload capability, readiness, and affordability. The alternatives

were scored on a scale from 1 to 5 for these metrics of interest, 5 being the best and 1 being the worst. Each alternative began at a value of 3 for each metric of interest and was adjusted accordingly with discussion among the team members as seen in Table 5. The scores were totaled for each alternative and the highest ranked alternatives were assessed to configure a preferred aircraft concept. The chosen alternatives are highlighted below.

Table 5: Scoring Matrix of Alternatives

Alternatives	Takeoff/Landing Performance	Survivability / Maneuverability	Payload Capability	Readiness	Affordability	SUM
Payload						
Wing Hardpoints	3	3	4	3	3	16
Fuselage Hardpoint(s)	3	3	4	3	3	16
Internal Bomb-bay	5	5	3	3	2	18
Gun Armament						
Centerline Cannon	3	3	2	3	2	13
Centerline MG(s)	4	4	3	3	4	18
Wing Mounted MG(s)	4	2	3	3	3	15
Wing Location						
Low	4	4	2	3	3	16
Mid	3	3	3	3	3	15
High	4	2	4	3	3	16
Wing Sweep						
None	4	3	3	3	5	18
Slight	2	4	3	3	1	13
Wing Dihedral						
None	4	3	3	3	4	17
Slight	2	4	3	3	2	14
Taper						
None	3	3	3	3	5	17
Slight	4	4	4	3	1	16

Alternatives	Takeoff/Landing Performance	Survivability / Maneuverability	Payload Capability	Readiness	Affordability	SUM
Wing Tilt						
Fixed Level	3	3	3	3	3	15
Slight Fixed Tilt	4	2	3	3	2	14
Variable Tilt	5	4	3	2	1	15
Pitch Effector						
Conventional Horizontal Tail	4	5	4	3	3	19
V-Tail	2	1	3	3	4	13
Yaw Effector						
Conventional Vertical Tail	4	5	4	3	3	19
Dual Vertical Stabilizer	3	4	2	3	2	14
V-Tail	2	1	3	3	4	13
Propulsor Location/Number						
Nose Mounted (1 engine)	3	2	3	3	5	16
Wing Mounted (2 engines)	5	4	3	3	2	17
Propulsor Type/Fuel						
Turboprop/Turboshaft (liquid)	5	3	3	5	5	21
Hybrid electric (liquid & batteries)	3	4	3	1	2	13

VII.B Preferred System Concept

Analysis of the scoring matrix of alternatives led to the consideration of two possible designs: a single-engine nose-mounted turboprop, fixed wing aircraft or a twin-engine wing-mounted turboshaft, tiltwing aircraft. The team identified the risk of designing a less affordable, tiltwing aircraft relative to a fixed wing aircraft but was concerned about offering something different then the A-29 and the AT-6. Both of these comparator aircraft meet the major requirements, have been tested, and are already in production. The RFP specifically mentions the

importance of flexibility in the design as military missions today are often unlike those tomorrow. For example, a tiltwing could be used in a search and rescue operation where landing is near impossible. Identifying the potential environments in which a light attack aircraft would likely be used led to further justification for versatility. Rugged, mountainous terrain in areas like Afghanistan will still make takeoff and landing difficult even if it can be performed in under 4000 ft, especially considering a majority of airfields in Afghanistan are under 2,500 ft in length [16]. Designing a tiltwing aircraft could offer some advantages to compete with the A-29 and AT-6 with justification as to why it might be a better light attack aircraft as opposed to more of the same. The team wanted to provide a new, unique solution to the light attack aircraft problem that felt worth designing as opposed to making an aircraft with slight performance and sizing differences to existing baseline aircraft. The tiltwing aircraft essentially combines the best aspect of an attack helicopter in achieving vertical takeoff and landing while still offering the ability for fast and efficient air travel. In comparing a tiltwing to a tiltrotor aircraft such as the V-22 Osprey, the tiltwing reduces interference caused by thrust hitting the wing when the rotors are in an upright or VTOL position. Additionally, a tiltwing aircraft can transition from VTOL to horizontal flight from zero forward velocity whereas a tiltrotor aircraft needs to be flying forward like a helicopter before transitioning [17]. One disadvantage of a tiltwing is reduced efficiency in hover mode, however the benefits of a tiltwing outweigh this drawback as the aircraft would most likely not be hovering for long periods of time during the design or ferry mission.

In order to counteract any added expense due to increased complexity of the tiltwing design, other features of the aircraft were simplified to maintain affordability such as including a conventional tail. The wing would have a straight and rectangular planform with no taper, sweep, or dihedral to keep manufacturing cost to a minimum as well as provide structural integrity for the wing. A high wing position was needed to complement the tiltwing allowing for proper clearance of the engines when grounded. High wing aircraft provide more stability in roll with better visibility for a ground-support aircraft but are less maneuverable. This tradeoff was accepted to achieve VTOL capability. Moving the engines to the wing also complemented positioning the integrated machine gun on the centerline in the nose of the fuselage, a feature which is notably preferred by pilots for accuracy relative to wing mounted machine guns. The loss of hardpoints on the wing due to wing mounted engines also resulted in the decision to use an internal bomb bay in the fuselage. The internal bomb bay should provide reduced radar signature and improved drag characteristics. A hybrid electric design was abandoned because of the need for TRL 8 by 2025, especially considering a non-conventional wing configuration was chosen. The team was concerned about the

readiness level of a tiltwing aircraft; however, the technology has been seen on various experimental aircraft as early as the 1960s such as the Canadair CL-84 Dynavert and the LTV XC-142.

VIII. Sizing Analysis

VIII.A Similarity Analysis

Although the A-29 and the AT-6 are the most equipped aircraft to meet the light attack aircraft RFP, the CL-84 was used as the primary seed aircraft for the design because it is in fact a tiltwing configuration with similar size and weight to the A-29 and AT-6. Key physical parameters for these three aircraft as well as the Kestrel are summarized in Table 6 [4-11].

Table 6: Comparator Data

Aircraft	Length (ft)	Height (ft)	Wingspan (ft)	Wing Area (ft^2)	Aspect Ratio	Empty Weight (lbs)	Gross Weight (lbs)	Engine SHP
Kestrel	40	15.6	35	245	5	8549	14,170	1870
CL-84	47.29	14.25	34.25	233.3	6.81	8417	14,500	1500
A-29	37.33	13	36.58	209	5.71	7055	11,905	1600
AT-6	33.33	10.66	34.12	178.7	5.24	5889	10,000	1600

VIII.B Initial Sizing and Constraint Analysis

An initial estimate of weight was found by using the takeoff gross weight (TOGW) estimation algorithm in Chapter 5 of *Fundamentals of Aircraft and Airship Design (2010)* by Leland Nicolai and Grant Carichner [18]. The TOGW or W_{TO} was defined as follows

$$W_{TO} = W_{fuel} + W_{fixed} + W_{empty} \quad (1)$$

where W_{fuel} is the total fuel weight required to perform the mission, W_{fixed} is the payload including crew, armaments, etc. and W_{empty} is the structure, propulsion, subsystems, avionics, etc. The algorithm was coded with the programming language, MATLAB, and proceeded as follows [19]

1. Pick a W_{TO}
2. Compute W_{fixed} based on design mission crew, payload, etc.
3. Estimate W_{fuel} using segment fuel fractions based on mission design
4. Compute $W_{empty_{avail}}$ as $W_{empty_{avail}} = W_{TO} - W_{fuel} - W_{fixed}$
5. Compute $W_{empty_{req}}$ using historical data/trends
6. Compute $W_{empty_{avail}} - W_{empty_{req}}$; Iterate on W_{TO} until $W_{TO}^{new} - W_{TO}^{old} < \epsilon$

The equation for empty weight of a tiltwing aircraft was determined using historical data of the CL-84 and the XC-142 [17]. The results of the algorithm can be seen in Figure 5.

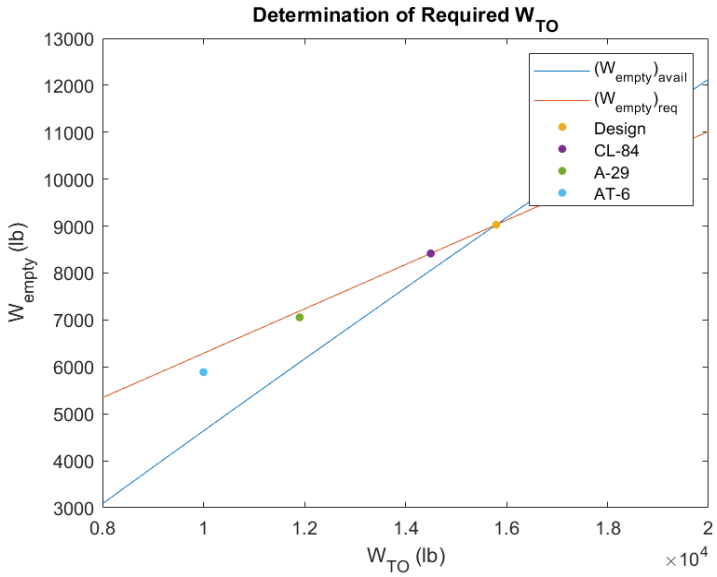

Figure 5: Initial Estimation of TOGW

The constraints of stall speed, takeoff and landing distance, cruise condition, climb condition, and service ceiling were determined using the specifications in the RFP and the initial estimate of size using equations from Nicolai and Carichner as well as an overview of conceptual design tools from Linköpings Universitet [20]. Hover

efficiency and vertical takeoff and landing (VTOL) capability constraints were added to aid in defining the design space for a tiltwing aircraft. For a tiltwing aircraft, a wing loading to disc loading ratio of 0.6 is an important design requirement [21]. Its function is to ensure a high velocity propeller slipstream over the wing which improves the stall characteristics of the wing during accelerating and decelerating transitions. The range of disc loading for proper vertical lift efficiency for a tiltwing is approximately 20 to 100 lb/ft^2 as seen in Figure 6 [22]. For reference, the CL-84 has disc loading of 39.9 lb/ft^2. To possess VTOL capability, the aircraft must have a thrust loading (T/W) of at least 1.

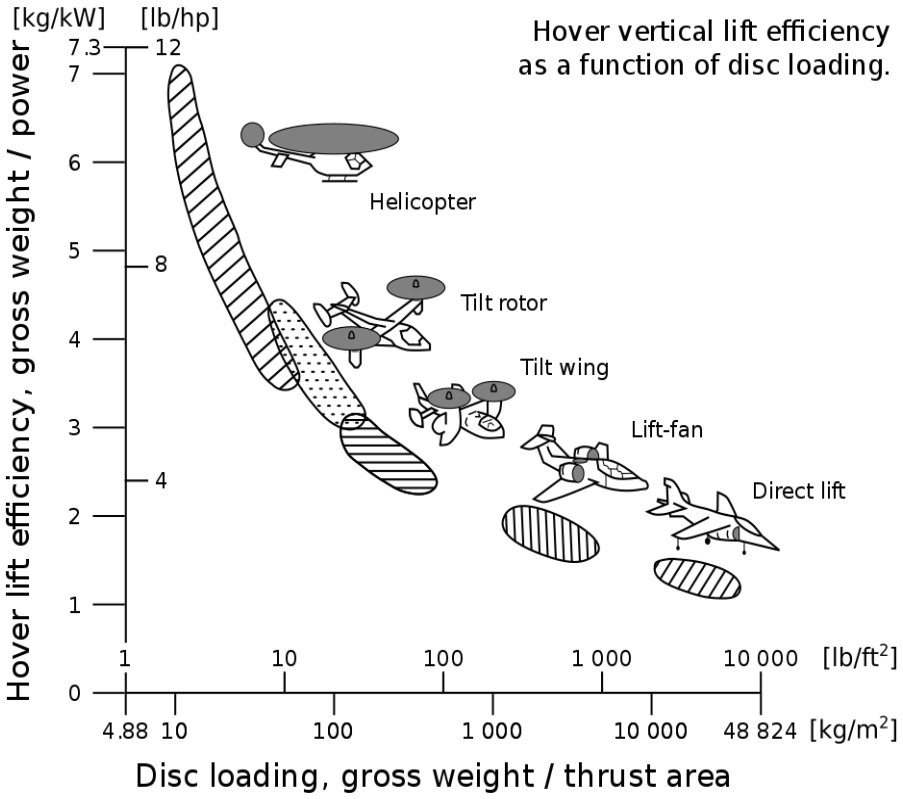

Figure 6: Range of Disc Loading for Tiltwing Aircraft

Figure 7 shows the feasible solution space for the light attack tiltwing aircraft. The blue cross marks the match point that was used to determine an initial optimum wing and thrust loading of approximately 58 lb/ft^2 and 1.05 respectively.

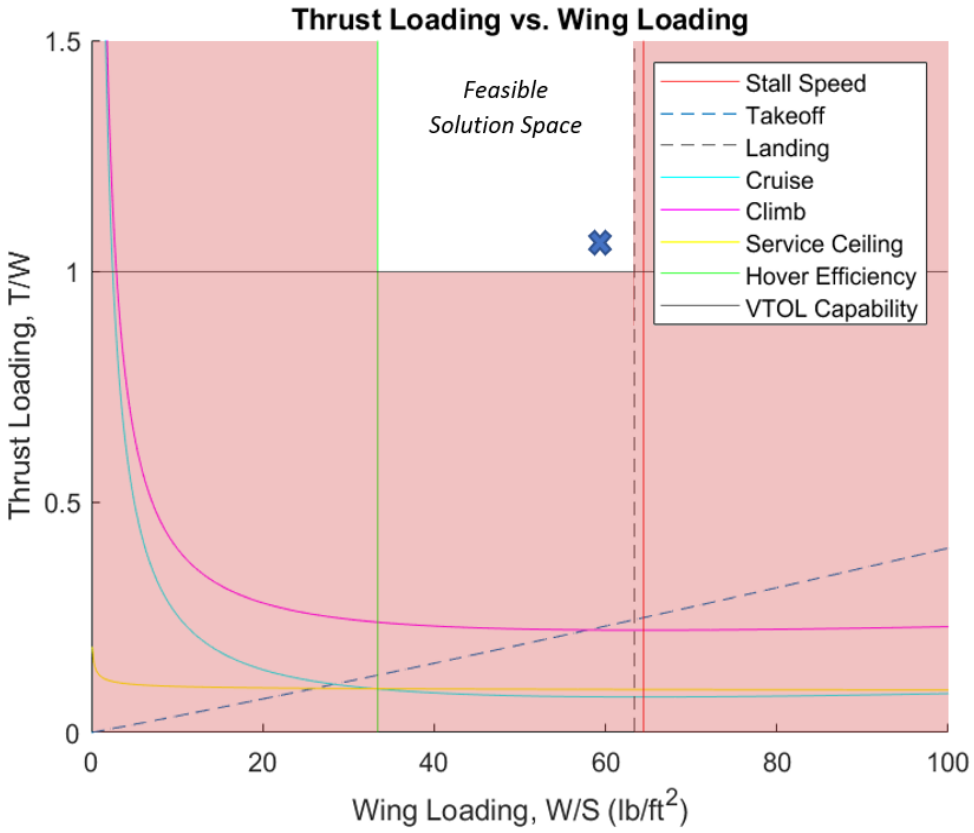

Figure 7: Carpet Plot

VIII.C Trade Studies

A weight sensitivity analysis was performed to determine the growth factors associated with payload weight and mission radius. In order to compute the relationship between W_{fixed} and W_{TO}, W_{fixed} was altered manually in MATLAB while the radius for the design mission remained constant. Alternatively, to compute the relationship between mission radius and W_{TO}, the radius was altered manually in MATLAB while the W_{fixed} remained constant. The corresponding values of W_{TO} were recorded in Microsoft Excel and plotted. A linear regression was performed to determine the sensitivity ratios, which can be seen in Figure 8.

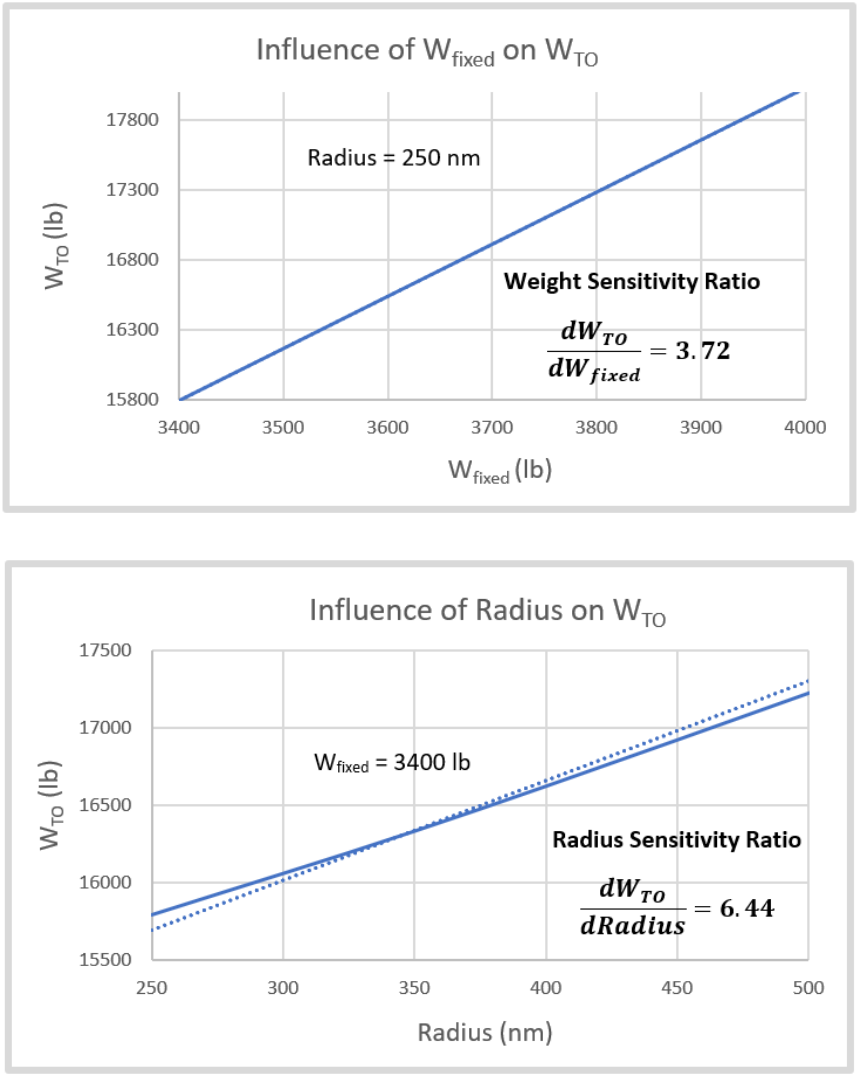

Figure 8: Growth Factors

A ground run distance trade study was conducted using guidance from *Introduction to V/STOL Airplanes (1981)* by David L. Kohlman, where VSTOL is defined as vertical and/or short takeoff and landing [23]. Two questions of interest were explored: what is the optimum thrust angle to minimize takeoff distance and what is the maximum possible reduction in takeoff ground run by thrust vectoring? Their relationships with thrust loading can be seen in Figure 9.

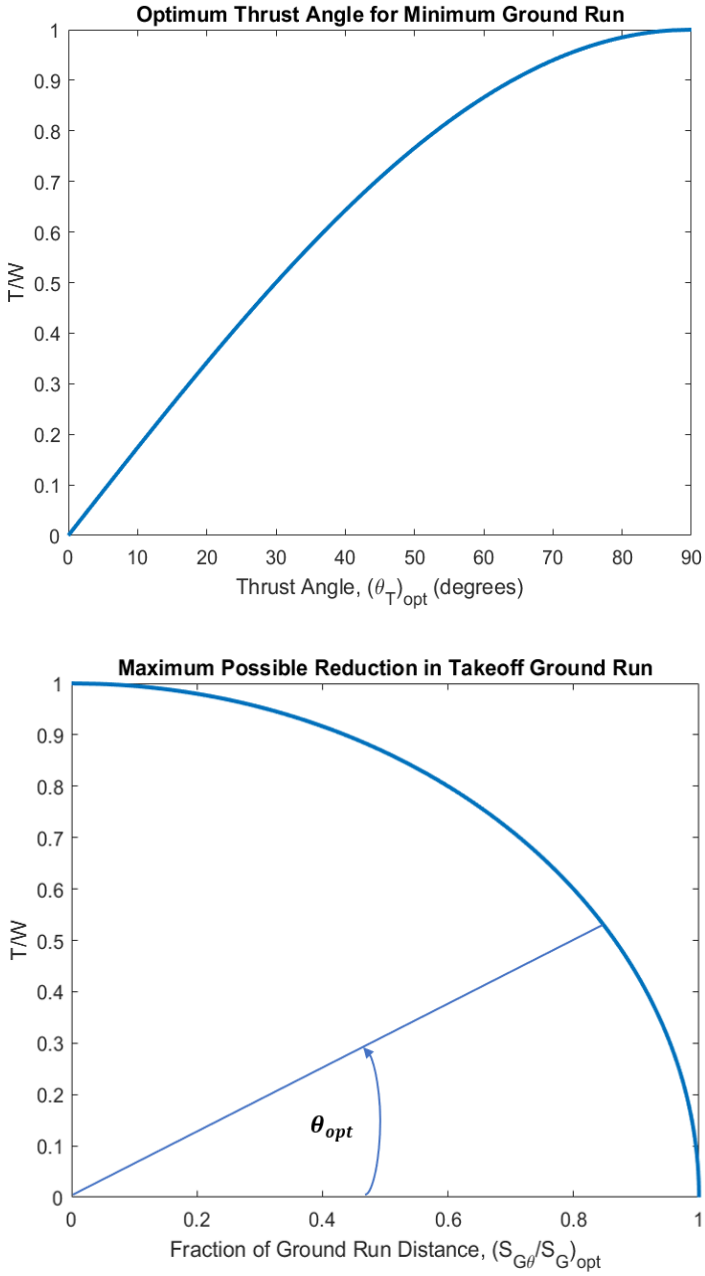

Figure 9: Thrust Vectoring

Unless the thrust loading (T/W) is very large, the reduction in ground run distance is quite small. In order to drastically improve the takeoff and landing distance relative to comparator aircraft like the AT-6 and the A-29, a more powerful engine must be selected, trading capability for added cost.

IX. Weight Summary

IX.A Refined Weight Estimate

A refined weight estimation for each of the components of the Kestrel can be seen in Table 7 on the next page. The weights were estimated using a combination of methods and equations from Chapter 20 of Nicolai and Carichner, an *Analysis of VSTOL Aircraft Configurations for Short Haul Air Transportation Systems (1966)* by R. Gallant, M. Scully, and W. Lange, and NASA's Flight Optimization System (FLOPS) software [18] [21] [24]. The VSTOL analysis was published by the Massachusetts Institute of Technology (MIT) Flight Transportation Laboratory and was consulted as a necessary source for guidance on tiltwing aircraft design. FLOPS is a system of computer programs developed at NASA to support aircraft design, sizing, and performance analysis. A SolidWorks 3D CAD model was specifically used to estimate the weight of the wing including internal structure such as spars and ribs as well as the cross shaft and pivot design for the tiltwing [25]. The weight was confirmed using FLOPS, the MIT report, and by multiplying the wing weight equation in Nicolai and Carichner by 15% to account for additional weight added due to the complexity of the wing design. The other components of the aircraft were averaged between various sources to improve accuracy of the Kestrel's final weight statement. If the weight estimate for each component was not within an order of magnitude and not close to the values calculated from other sources, or was unavailable, it was omitted from being used in the average estimation. Various specifications sheets found online from manufacturers were used for known components on the market, such as the GE T700 engine [26].

Table 7: Aircraft Component Weight Estimation

Component	Source	Weight (lb)	Percentage
Wing	Nicolai, FLOPS, Gallant, SolidWorks	1106	7.8
Horizontal Tail	Nicolai, FLOPS	114	0.8
Vertical Tail	Nicolai, FLOPS	99	0.7
Fuselage	Nicolai, FLOPS	1140	8.0
Landing Gear	Nicolai, FLOPS	545	3.8
Nacelle (Air Induction)	FLOPS, Gallant	197	1.4
Structure Total	-	**3200**	**22.6**
Engines	GE T700 Spec. Sheet	986	7.0
Propellers	Nicolai, Gallant	1045	7.4
Transmission (Gearbox)	Nicolai, Gallant	327	2.3
Misc. Systems	FLOPS	121	0.9
Fuel System	Nicolai, FLOPS	514	3.6
Propulsion Total	-	**2993**	**21.1**
Surface Controls	Nicolai, FLOPS, Gallant	520	3.7
Auxiliary Power	FLOPS	269	1.9
Instruments	Nicolai, FLOPS	79	0.6
Hydraulics	FLOPS, Gallant	124	0.9
Electrical	FLOPS, Gallant	359	2.5
Avionics	Nicolai, M-130 Spec. Sheet	594	4.2
Furnishings and Equipment	FLOPS, Gallant	305	2.1
Air Conditioning	FLOPS, Gallant	106	0.7
System and Equipment Total	-	**2356**	**16.6**
Weight Empty	-	**8549**	**60.3**
Crew and Baggage	FLOPS, Gallant	415	2.9
Unusable Fuel	FLOPS	144	1.0
Engine Oil	FLOPS	49	0.3
Operating Empty Weight	-	**9157**	**64.6**
Armament	Various Spec. Sheets	3000	21.2
Zero Fuel Weight	-	**12157**	**85.8**
Mission Fuel	FLOPS	2013	14.2
Gross Weight	-	**14170**	**100.0**

IX.B Avionics

The specific list of avionics used on the Kestrel can be seen in the Table 8. Chapter 8 of Nicolai and Carichner was primarily used for selection of the avionics components for a light attack aircraft and as a source for associated weight values. The necessities for any aircraft were chosen first including communications, navigation, autopilot, and a flight data recorder. Avionics that fit the light attack aircraft class were then included such as a countermeasure dispenser, heads-up display (HUD), radar, and a gun camera among others. The M-130 countermeasure dispenser weight was found online [27]. The following abbreviations in the table are defined as ultra high frequency (UHF), direction finding (DF), identification friend or foe (IFF), tactical air navigation system (TACAN), instrument landing system (ILS), and very high frequency omni-directional range (VOR).

Table 8: Avionics Equipment

Item	Weight (lb)
UHF Communications	11
UHF DF horning	11
Air-to-ground IFF	13
TACAN	46
ILS-VOR	4
Gyrocompass	8
Inertial navigation system	44
High-frequency radio	78
Autopilot system	169
Air data computer	14
2x M-130 Countermeasure Dispenser	56
Radar altimeter	38
Range-only radar	25
Radar warning and horning	22
Heads-up display	37
Gun camera	2
Flight data recorder	16
Total	**594**

IX.C Payload and Fuel System

A complete list of armaments that make up the 3000 lb payload requirement as well as the allocation of fuel can be seen in Table 9. The weight values for the armaments were found online in specifications sheets [28-33]. The Kestrel stores JP-4 type fuel in bladder tanks, with primary fuel storage in the wing and reserve fuel storage in the fuselage. The following abbreviations in the table are defined as air-to-ground (AGM), folding fin aerial rocket (FFAR), and forward-looking infrared (FLIR).

Table 9: Payload and Fuel Allocation

Item	Weight (lb)
2x AGM-65 Maverick Missile	462
MK-82 Bomb	500
2x LAU-68 F/A Rocket Launcher	184
14x MK-4 FFAR Mighty Mouse Rockets	259
FLIR Star Safire II	119
Chaff and Flares	30
M-197 20 mm Gatling Gun	132
4500x 20 mm Rounds of Ammunition	1314
Payload Total	**3000**
Primary Fuel Capacity	2000
Reserve Fuel Capacity	250
Total Fuel Capacity	**2250**

The armaments were selected by assessing the munitions carried by current light attack aircraft such as the A-29 and the AT-6 with consideration for the RFP objective to possess provisions for carrying/deploying a variety of weapons, including rail-launched missiles, rockets, and 500 lb (maximum) bombs. With the configuration above, the machine gun has enough ammo to fire for approximately three minutes of continuous fire. After research into the A-10 Warthog, the time allowed per strafe to fire on an enemy target is approximately two seconds [34]. Knowing this, this aircraft can accomplish approximately 90 passes with the ammo provided in Table 9. This is believed to be an adequate amount for the time that the plane must remain on station circling. This can change however, as

multiple configurations of armaments can be utilized by this aircraft. This configuration features an air-to-ground CAS focused loadout, but serves as an example of the near limitless potential configurations this aircraft offers. The Kestrel could alternatively be outfitted with other armaments such as the AIM-9L Sidewinder air-to-air missile by adjusting the ammunition and payload carried.

IX.D Center-of-Gravity Envelope

The Kestrel's center-of-gravity (C_g) location was measured relative to the nose of the aircraft. The C_g travel is depicted in Table 10 for various load conditions of the aircraft. The furthest forward aerodynamic center is 17.16 ft. This gives a most aft C_g for safe flight of 17.02 ft (considering a minimum SM of 2%). The most forward C_g for safe flight is established as 14.25 ft.

Table 10: Variation of C_g Dependent on Load Condition

Aircraft Condition	C_g Location from Nose (ft)	Static Margin (%MAC) > 2%
Reserve Fuel - Zero Payload	14.25	41.6
Max Fuel - Zero Payload	14.5	38.0
Max Fuel - Max Payload	14.7	35.1
Reserve Fuel - Max Payload	14.25	41.6
50% Fuel - Rear Payload	14.8	33.7
Average CG	14.5	38.0

X. Aerodynamics

X.A Airfoil Selection and Wing Design

The airfoil selected for the aircraft is the NACA 63(3)-418 airfoil, which can be seen in Figure 10. This airfoil was used on the CL-84, a similar sized aircraft with respect to wingspan, wing area, and weight. Additionally, it has aerodynamic properties that benefit the tiltwing design. The NACA 63(3)-418 worked effectively to postpone stall to higher angles of attack than available with most conventional airfoils when tested for the CL-84 [35]. For the design of the wing, the team chose a straight and rectangular planform. This will help to keep wing manufacturing to a low cost as the ribs will all be the same size and shape. A tapered wing was considered for possible weight reduction and improved aerodynamic characteristics, but the nonuniform ribs would have led to more expensive wing. The wing also has a large wing area, with the wingspan of 35 ft and a chord of 7 ft. This large chord provides necessary space to house fuel and strengthens the structural integrity of the wing. The wing's internal structure houses four fuel tanks and must be strong enough to carry the engines. There is enough space within the wing to hold 42.8 cubic feet of fuel, which equates to approximately 2000 lbs of JP-4 fuel according to Chapter 8 of Nicolai and Carichner [18].

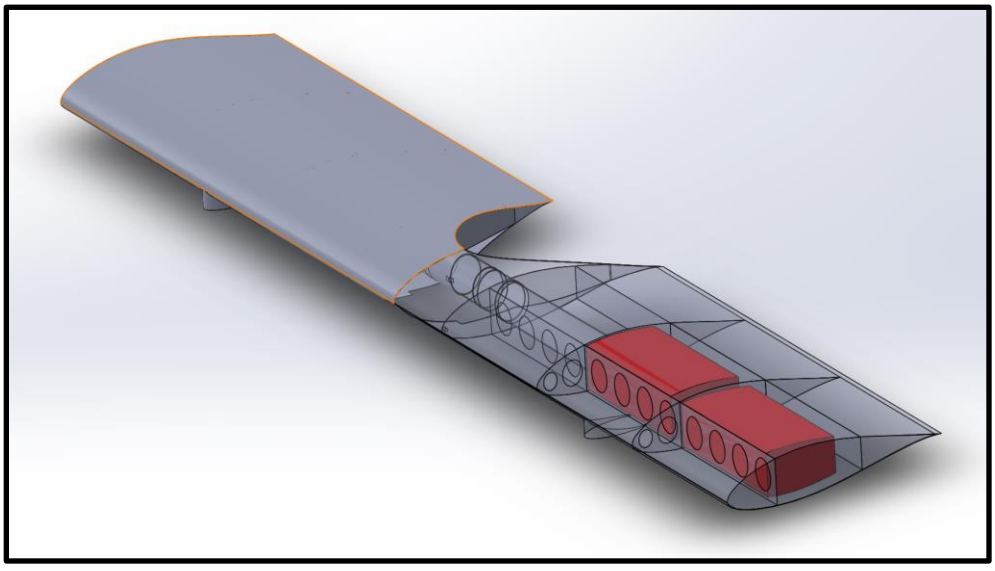

Figure 10. NACA 63(3)-418 and Fuel Storage

X.B Aerodynamic Characteristics

Table 11: Aerodynamic Characteristics of Required Flight Segments

Segment	Mach	Altitude (ft)	C_L	L/D	SFC
Design Cruise	0.5	10,000	0.20	10.0	0.43
Loiter	0.27	3,000	0.53	12.3	0.30
Ferry Cruise	0.39	18,000	0.37	12.9	0.36

Looking above at Table 11, loiter was specifically optimized to minimize fuel flow and maximize aircraft endurance. Also, as Mach increases across each segment of mission, the coefficient of lift (C_L) goes down. These numbers were computed internally within FLOPS's aerodynamics module, which makes use of a modified version of the Empirical Drag Estimation Technique (EDET). They were checked for accuracy using VSPAero, the aerodynamics solver within openVSP, and DARcorporation's FlightStream Aerodynamic Modeling Software [36]. The specific fuel consumption (SFC) in this table is accurate for the GE T700 engine according to specification sheets found online.

Table 12: Parasitic Drag Buildup

Component	Cd0	Percentage (%)
Fuselage	0.0053	11.2
Horizontal Stabilizer	0.0022	4.7
Vertical Stabilizer	0.0010	2.1
Landing Gear	0.0150	31.8
Wing	0.0091	19.3
Engines	0.0146	30.9
Total	0.0472	100.0

When calculating the parasitic drag buildup in Table 12, the aircraft was analyzed for short takeoff and landing (STOL) with a wing angle of 25 degrees. A wing angle of 25 degrees was chosen because of the need for propeller clearance when grounded. These numbers were all computed in VSPAero, and were checked in both

FlightStream and FLOPS. The only value not computed in VSPAero is the coefficient of drag for the landing gear, which was estimated with data from Nicolai and Carichner.

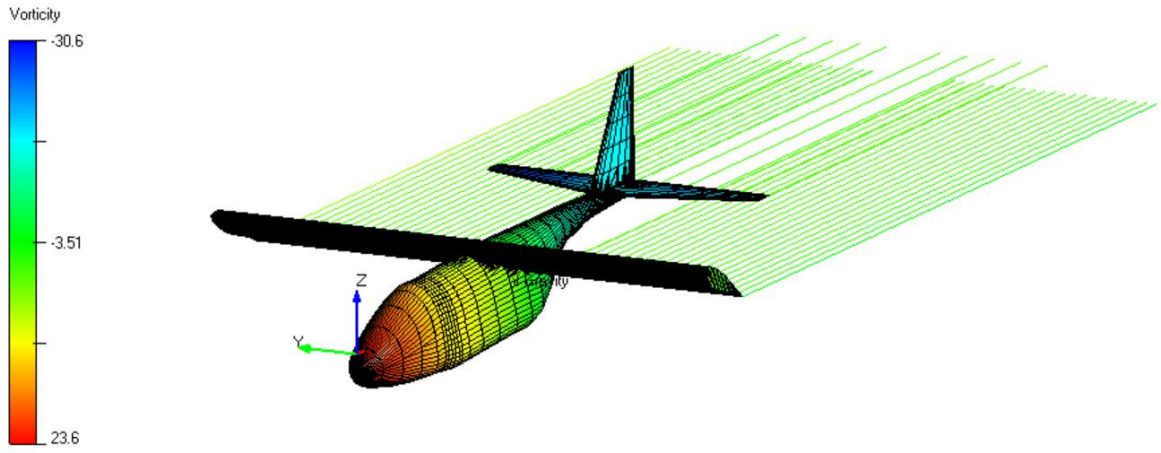

Figure 11: FlightStream Simulation Example 25° Wing Angle

X.C High Lift Device

The high-lift system on the aircraft will be geared flaps as pictured in Figure 12. These flaps are similar to single slotted flaps, however single slotted flaps have a limited range of motion and only move to specified angles. By using geared flaps, the Kestrel's pilot will be able to operate flaps in a full range of motion. This is important because the geared flaps are needed for pitch control of the aircraft, serving as a substitute for a tail rotor.

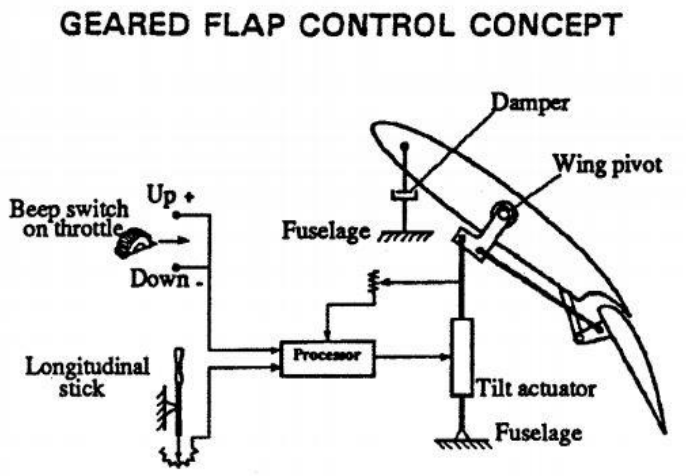

Figure 12: Geared Flap Schematic [37]

The geared flap allows for direct pilot manipulation of the flaps, which directs the flow from the rotors. The geared flap concept has been flight tested in the 1970s and was controllable. With modern computer-aided stabilization, this method of pitch control can be greatly improved. By utilizing mechanisms that are already on board the aircraft with minor modifications, the desired capabilities for control can be created without adding unnecessary weight or more complexity associated with a cyclic or additional rotor.

X.D Computation of CL_{max}

The rotation of the wing during takeoff and landing drastically affects aerodynamic characteristics such as lift and drag. The maximum coefficient of lift ($C_{L_{max}}$) of the aircraft needed to be determined at various wing tilt angles to accurately predict STOL performance. The relationship between $C_{L_{max}}$ and wing tilt angle was computed in MATLAB using the methods outlined in *Aerodynamics of V/STOL Flight (1967)* by Barnes W. McCormick [38]. The significant angles involved in a wing-propeller combination are depicted in Figure 13.

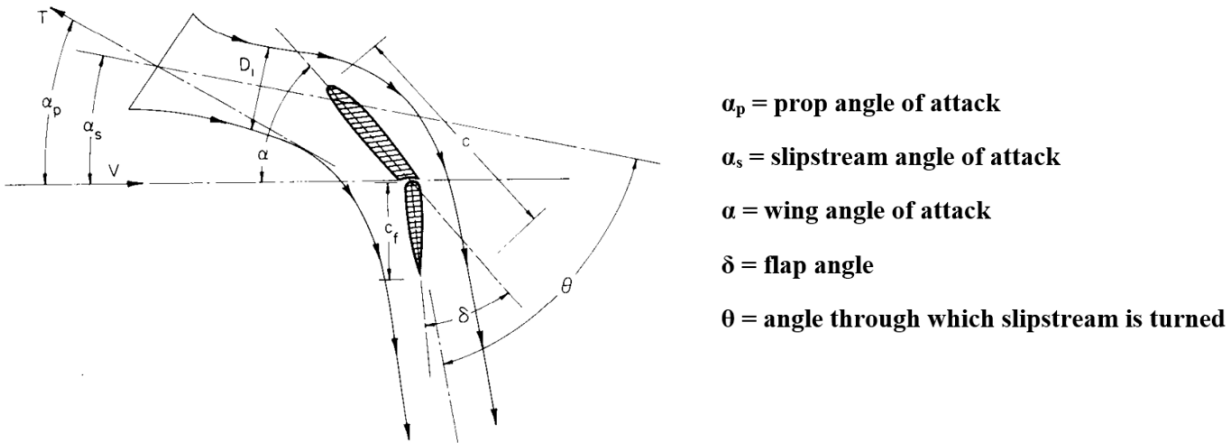

Figure 13: Wing-Propeller Combination

The total coefficient of lift (C_L) for each wing tilt angle can be seen in Equation 2. $C_{L_{T=0}}$ signifies the lift that the wing would produce without the propeller. $C_{L_\Gamma}$is indicative of the lift that results from the additional circulation produced by the effect of the slipstream acting as a jet flap on the flow external to the slipstream. $C_{L_{prop}}$ represents the vertical component that results from the turning of momentum in the slipstream.

$$C_L = C_{L_{T=0}} + C_{L_\Gamma} + C_{L_{prop}} \quad (2)$$

C_L must also be reduced by the vertical component of the profile drag of the wing immersed in the propeller slipstream. Thus, Equation 3 was used to compute the $C_{L_{max}}$ of the wing at various tilt angles.

$$C_L = C_{L_{T=0}} + C_{L_T} + C_\mu sin(\alpha_s + \theta)(\frac{sin(\alpha_p)}{sin(\alpha_s)} - \frac{D}{T}) \quad (3)$$

$C_{L_{T=0}}$ and drag were found using data from a VSPAero analysis of the NACA 63(3)-418 airfoil. Thrust was estimated using a FLOPS engine deck from a GasTurb model of the GE T700 engine/rotor system. Modeling of the propulsion system will be covered in the next section. The remaining lift components were calculated by assuming constant flap angles of 15° and 30° for takeoff and landing respectively, and by alternating the angle of attack of the wing. The final results of the analysis can be seen in Figure 14.

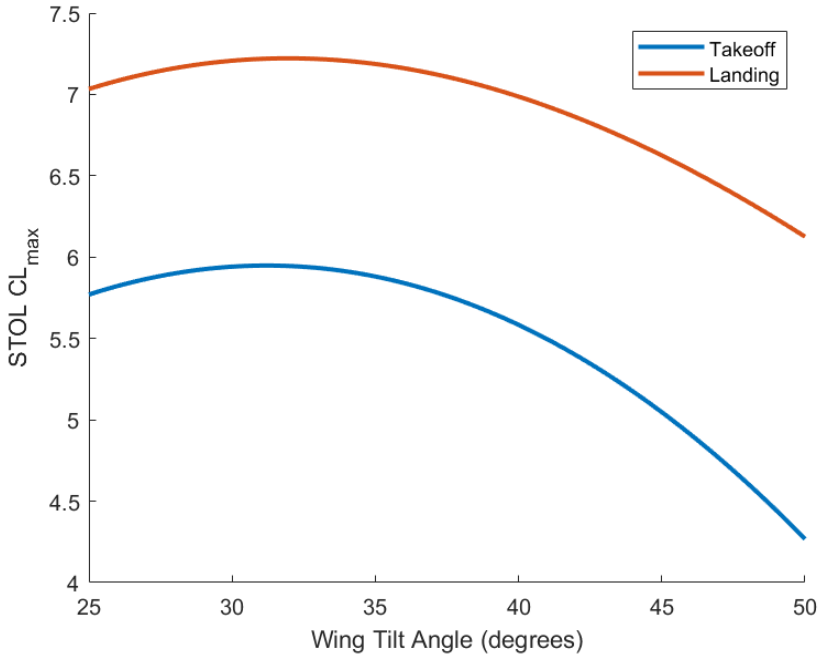

Figure 14: $C_{L_{max}}$ as a Function of Wing Tilt Angle

The $C_{L_{max}}$ for takeoff was found at a wing tilt angle of 31° to be 5.95 while the $C_{L_{max}}$ for landing was found at a wing tilt angle of 32° to be 7.22. Ideally, the flap angle could be changed while tilting the wing via pilot control to maximize the lift generated for best STOL performance.

XI. Propulsion

XI.A Engine Type Down-Select

The first step in designing an effective propulsion system for the Kestrel was deciding what class of engine to select. There are a variety of different engine classifications used in both military and commercial aircraft, with each offering benefits and drawbacks which needed to be analyzed with respect to the RFP and mission profile. Broadly speaking, there are four main engine types used for aircraft propulsion: turboprop/turboshaft, turbofan, turbojet, and electric aircraft propulsion (EAP). For this design project, two of these were given serious consideration for a potentially suitable propulsion system, those being the turboprop and turbofan. A turboprop engine offered generally higher efficiency values and a quieter noise profile, both favorable traits for an affordable and survivable light attack aircraft. On the other hand, while not quite at the level of a turboprop, turbofan engines still offered competitive efficiency values relative to other propulsion systems, while offering significantly greater thrust outputs than comparably sized turboprop engines. Although briefly explored, both turbojets and EAP were deemed unsuitable for the design requirements and not given any meaningful consideration for the project. While turbojets were a staple of military aircraft propulsion in the mid-1900's, the development of turbofans have led to them being nearly entirely phased out as a propulsion system in the modern air fleet, as they offer next to no tangible advantage over a turbofan engine, save for slightly less complexity in design. EAP did offer the potential for a propulsion system far quieter than even a turboprop could provide, but this technology is still in the relatively early stages of development. Doubt was cast over the ability of modern battery technologies to effectively store the necessary power for the mission profile, especially given the 2025 entry date. Furthermore, the infrastructure of military air bases and aircraft maintenance would require notable change to accommodate an electric powered aircraft, and in combination with concerns over the durability of EAP in austere frontline conditions, EAP was not pursued for this project.

To decide between a turboprop or turbofan engine, the target design parameters for altitude and cruising speed were consulted and compared to existing literature on the relative operating profiles of various engine classes. From the RFP, the aircraft must have a service ceiling of 30,000 ft or greater, and from the design and ferry mission breakdowns, a conservative requirement for cruise capability was estimated at 300 kts. Using these values for altitude and airspeed, this target operating region was plotted on Figure 15 shown below. Figure 15 comes from

Chapter 4 of Nicolai and Carichner, and plots the service regions of various propulsion systems relative to altitude and airspeed.

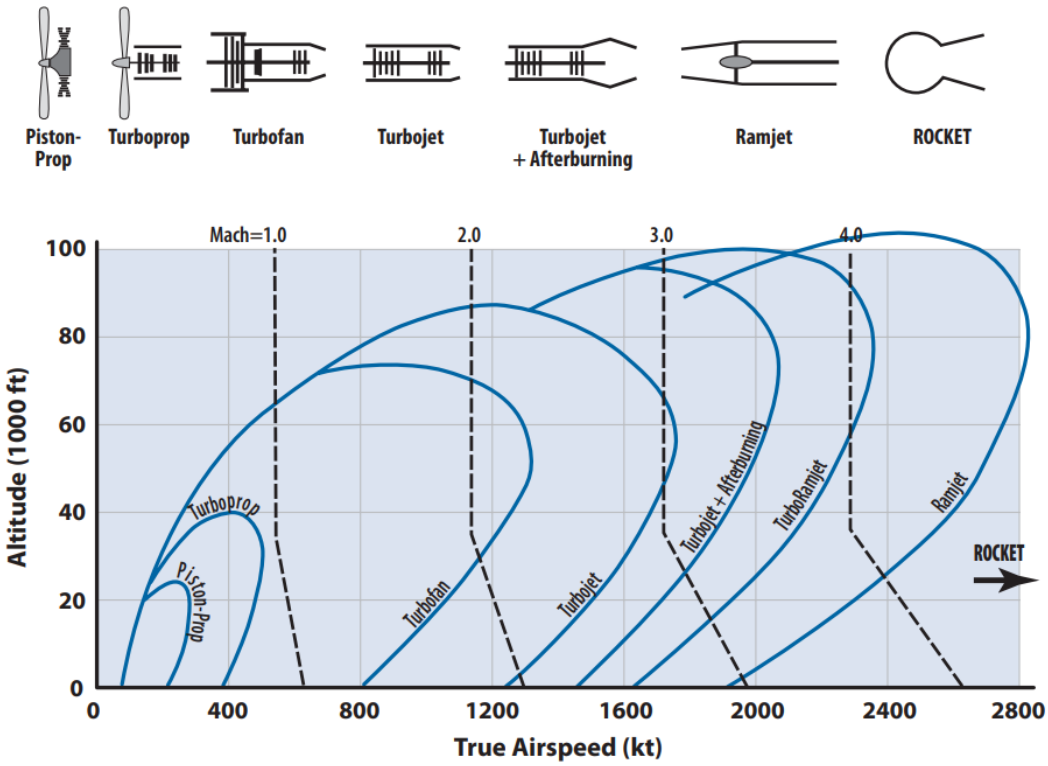

Figure 15: Service Regions for Various Propulsion Systems [18]

Looking at the plot, it is rapidly evident that piston-props would be insufficient for the design aircraft, while turbofans would likely be overqualified for the mission, providing excessive thrust, weight, and cost. Thus, it was decided that a turboprop propulsion system was the most feasible option, and any further engine sizing endeavors were done with a turboprop engine in mind.

XI.B Engine Sizing & Selection

Once the team decided to pursue a tiltwing configuration for the aircraft, it was apparent this would present additional challenges in sizing the propulsion system. Considerations for wing tilt angle and VTOL capability sizing would require unique sizing procedures, on top of the traditional methodology for a conventional takeoff and landing aircraft. To begin, existing literature on both tiltwings and helicopters was studied to better grasp where to

begin. Several existing and experimental tiltwing and tiltrotor aircraft were analyzed in order to formulate ballpark estimates for what a reasonable shaft horsepower requirement would be for a twin-engine aircraft with the Kestrel's expected TOGW. These included the Canadair CL-84, Kaman K16-B, Hiller X-18, LTV XC-142, and the V-22 Osprey. Based on these examples, a first guess for the ballpark shaft horsepower requirements per engine was placed at just above 2,100 shp. This provided a frame of reference as more precise engine sizing was initiated, allowing the team to gauge whether sizing was progressing in an expected manner.

The methodology used for sizing the Kestrel's propulsion system followed the steps performed by an MIT Flight Transportation Laboratory study for the Department of Aeronautics and Astronautics [21]. This paper focused on analyzing VSTOL aircraft configurations for short haul air transportation systems, and was deemed sufficiently comparable to the design project to serve as a primary methodology to size the turboprop engines. Another key assumption that was made prior to engine sizing was determining the VTOL takeoff gross weight, and how much it would differ from the full TOGW capacity. Early on in the propulsion study, it became apparent that having the capability to perform full VTOL at the maximum takeoff gross weight would require unfeasibly large and powerful engines relative to the aircraft and design mission, leading to severe complications in other aspects of aircraft weight, performance, and cost. As such, it was decided to size the aircraft for full VTOL at approximately 60% of the maximum TOGW. It was deemed this would still enable the Kestrel to have true VTOL capabilities at a reasonable payload capacity, while preventing required engine outputs from far surpassing the requirements for angled STOL, and with both angled takeoff and landing estimates still below 1,000 feet, this was viewed as an acceptable tradeoff.

The main variables which went into this engine sizing methodology were the takeoff gross weight, propeller tip speed, rotor rpm, and propeller diameter. Rotor design is explored in more detail in the following section, but with these main parameters along with a few others, a simple algorithm for sizing the engines was developed in MATLAB. To begin, a propeller thrust coefficient at hover was determined using Equation 4 below, where W_G is the takeoff gross weight estimate, NE is the number of engines (two), ρ_{SL} is the density at sea level, Ω is rotor rpm, and D is rotor diameter.

$$C_{T_{Hover}} = (W_G) \,/\, [NE \ * \ \rho_{SL} * (\Omega)^2 * (D/2)^2] \tag{4}$$

With this coefficient calculated, the next major steps were to calculate the horsepower required for hover conditions, and subsequently the shaft horsepower necessary. The horsepower was calculated using Equation 5

below, where V_{tip} is the tip speed of the propellers, $C_{D_{prop}}$ is the coefficient of drag of the propellers, and all other variables are previously defined.

$$HP_{Hover} = [\ (W_G)\ /\ (550 * C_{T_{Hover}})\ ] * V_{tip} * [\ C_{D_{prop}} + (C_{T_{Hover}}\ /\ \sqrt{2})^{3/2}] \quad (5)$$

This horsepower requirement was then converted into a shaft horsepower requirement by accounting for both the propeller efficiency and the transmission efficiency. Both of these values were set to a 90% efficiency based off the MIT study, leading to the final shaft horsepower requirement as shown in Equation 6 below, where η_{hover} is the propeller efficiency in hover and η_{trans} is the transmission efficiency

$$SHP_{Hover} = HP_{Hover}\ /\ (\eta_{hover} * \eta_{trans}) \quad (6)$$

Using this basic methodology, an initial sizing for the engine was established and iterated on as better calculations for TOGW, propeller characteristics, and other parameters were developed. After several refinements, a satisfactory SHP requirement of 1844 shp for each engine was reached, which would enable the aircraft to achieve VTOL at the target 60% takeoff gross weight goal. With a firm shaft horsepower need calculated, existing turboprop possibilities were explored, and it was ultimately decided to select the GE T700 turboshaft engine for the aircraft. The GE T700 engine is a proven platform currently in service on numerous US army aircraft and rotorcraft, notably the AH-64 Apache and UH-60 Black Hawk. The variant selected for the Kestrel, the GE T700/T6A1, can be seen in Figure 16 below, and key metrics of the engine are likewise summarized below in Table 13. Beyond simply meeting the shaft horsepower requirements calculated for the aircraft, the GE T700 boasted competitive SFC values and weight which made it a suitable option. Furthermore, adopting an existing and well-proven engine like the GE T700 helped to assuage durability concerns about how a newer or more fragile engine might fare in the rugged, austere environments this aircraft is expected to operate within. As a platform already in service with the armed forces, it is further hoped that implementing a familiar engine will help to keep costs and maintenance difficulties down, relative to selecting an engine being introduced to a military setting for the first time.

Figure 16: GE T700 Turboshaft Engine [26]

Table 13: Key Parameters of GE T-700/T6A1 [26]

Length	47 in
Nominal Diameter	15.6 in
Weight	493 lbs
Maximum Continuous SHP	1,870 shp
Maximum Continuous SFC	0.452
Intermediate SHP (30 mins)	2,145 shp
Intermediate SFC (30 mins)	0.445

Once a final engine was selected, the next step was to develop an engine deck for the combined turboshaft/rotor system to be used in mission analysis. This was conducted using the gas turbine performance simulation program, GasTurb, and MIT's propeller analysis tool, XROTOR [39] [40]. The design of the rotors will be covered in the next section. A model of the GE T700/rotor system was constructed within GasTurb, using data provided by GE, with missing parameters being filled in through other sources and baselines from comparable engines. Once this model was constructed, slight improvements were made to existing characteristics to account for incremental technological growth by the 2025 entry date. The GE T700 engine is soon to be replaced by the T901

engine on platforms such as the Apache and Black Hawk attack helicopters. For lack of data availability on the T901 engine as well as the need for a TRL 8, the best approximations involved analyzing and applying trends in advanced models of current turboshaft engines in the case of the T700. This took place primarily in slight component efficiency boosts, along with improved burner temperature capabilities. For example, polytropic efficiency of the T700 engine was assumed to improve by about 2% for an advanced model by 2025 using analysis from a NASA presentation on modeling turboshaft engines for vertical lift technology [41]. A sample output from GasTurb for a set altitude and Mach number can be seen below in Figure 17.

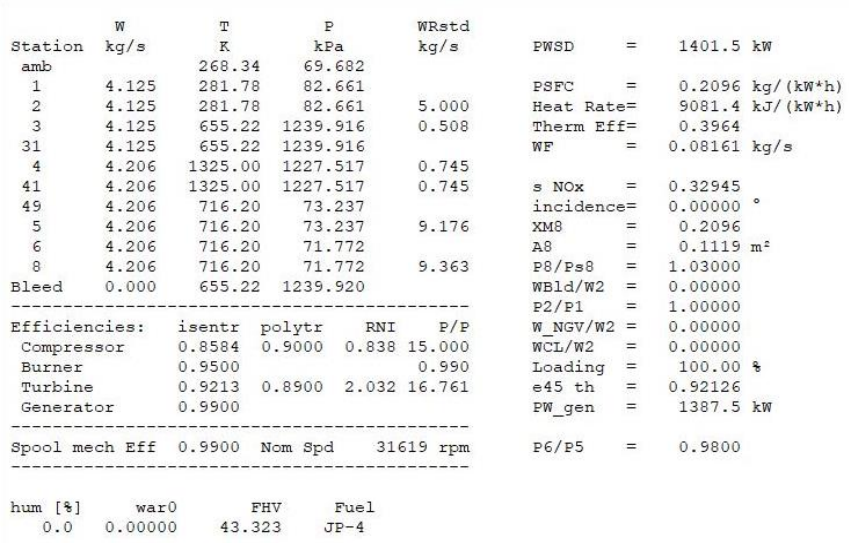

```
          W         T         P        WRstd
Station  kg/s       K        kPa       kg/s       PWSD     =    1401.5 kW
 amb               268.34    69.682
  1      4.125     281.78    82.661               PSFC     =    0.2096 kg/(kW*h)
  2      4.125     281.78    82.661     5.000     Heat Rate=    9081.4 kJ/(kW*h)
  3      4.125     655.22  1239.916     0.508     Therm Eff=    0.3964
 31      4.125     655.22  1239.916               WF       =   0.08161 kg/s
  4      4.206    1325.00  1227.517     0.745
 41      4.206    1325.00  1227.517     0.745     s NOx    =   0.32945
 49      4.206     716.20    73.237               incidence=   0.00000 °
  5      4.206     716.20    73.237     9.176     XM8      =    0.2096
  6      4.206     716.20    71.772               A8       =    0.1119 m²
  8      4.206     716.20    71.772     9.363     P8/Ps8   =   1.03000
Bleed    0.000     655.22  1239.920               WBld/W2  =   0.00000
-------------------------------------------       P2/P1    =   1.00000
Efficiencies:    isentr  polytr    RNI    P/P     W_NGV/W2 =   0.00000
 Compressor      0.8584  0.9000  0.838 15.000     WCL/W2   =   0.00000
 Burner          0.9500                0.990     Loading  =    100.00 %
 Turbine         0.9213  0.8900  2.032 16.761     e45 th   =   0.92126
 Generator       0.9900                          PW_gen   =    1387.5 kW
-------------------------------------------
Spool mech Eff  0.9900  Nom Spd    31619 rpm      P6/P5    =    0.9800
-------------------------------------------

hum [%]     war0       FHV      Fuel
   0.0    0.00000    43.323    JP-4
```

Figure 17: Sample Engine Output using GasTurb (Alt = 10,000 ft; M = 0.5)

Two additional points of note were brought up through team discussion with faculty advisors, with regards to a turboshaft engine on a tiltwing configuration. First, was the necessary inclusion of a gearbox for each turboshaft engine, to account for the design rpm of the engine being significantly lower than the factory capabilities of the GE T700. This resulted in approximately 600 lbs additional weight which was accounted for in the weight section, along with slight efficiency penalties which were accounted for in the sizing methodology and GasTurb model. The second point of note was the necessity of fuel system modifications within the engines themselves. Normally, an engine implemented into an aircraft is designed for either strictly horizontal flight (fixed wing aircraft) or strictly vertical flight (helicopter), and fuel and oil systems are designed accordingly. However, as a tiltwing design, the engines on the aircraft must be capable of transitioning between both orientations, necessitating these additional

considerations. Further analysis is needed to determine the exact manner this would manifest, but at a minimum it was noted that this would lead to increased costs and maintenance considerations.

XI.C Rotor Design

To design the rotors of the Kestrel, XROTOR was utilized to create a rotor design based on inputs given by the chosen GE T700 engine and guidance from the MIT VSTOL report. The largest contributions to this design showed itself in the thrust that the rotors needed to produce, the diameter of the rotors, and hub size. For VTOL at 60% payload, each engine needed to produce approximately one half of total weight which equals 6485 pounds of thrust. From the MIT VSTOL report, the diameter of the rotors was found to be 13.1 feet, the propeller tip speed about 608 mph, and the rotor rpm is approximately 400 rpm. The hub was then designed using estimations in the XROTOR user guide and information of the T700 to have a diameter of 1 foot and a hub wake radius of 0.2 feet to connect the rotors to the gearbox.

The last variable needed for the design of the rotors was the number of blades used. For weight considerations, it was decided to not go above four propellers on an engine. Knowing this, the trade study became between three and four propellers. The utilization of three propellers would slightly increase the efficiency of the aircraft as well as lower the overall weight of the aircraft. In comparison, the four-propeller configuration would increase the thrust as well as lower the overall sound profile due to the propeller tip. Understanding the differences between these two configurations, the four-propeller configuration was chosen mainly for noise and stealth reasons. As seen below in Figures 18 and 19, the ground decibel level at takeoff for the plane increases by approximately five decibels by using the three-propeller configuration as well as increasing the area that is affected by the max decibel level. This may not seem to be a significant difference, however it does have more of an effect on the range the plane can be heard from as will be explored later in this report.

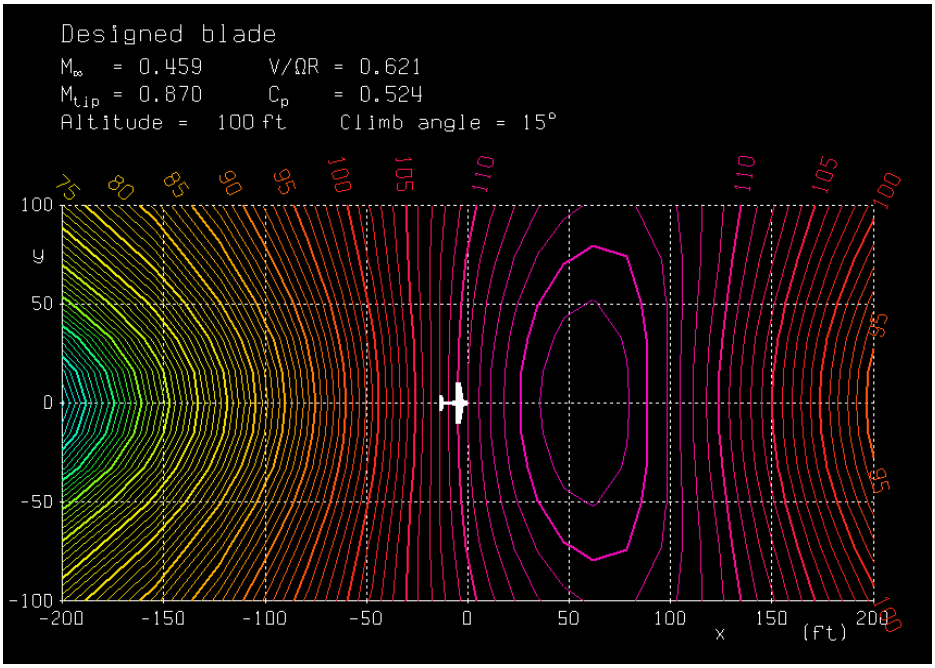

Figure 18: Four-Propeller Noise Profile at Takeoff

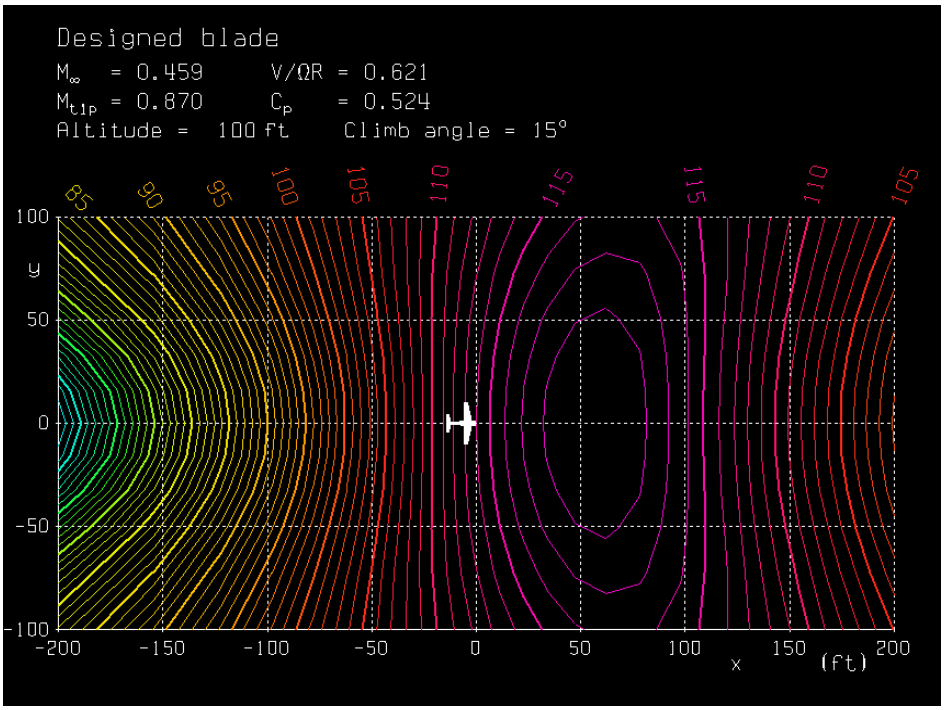

Figure 19: Three-Propeller Noise Profile at Takeoff

Taking all of these parameters into account, the final rotor design computed in XROTOR is shown in Figure 20. Notable features of this design include a twist of the propeller starting at the base and continuing

throughout the blade. Also, the blade is shown to have a fairly large area when shown in an untwisted shape. This rotor is able to produce the needed thrust of approximately 6845 pounds.

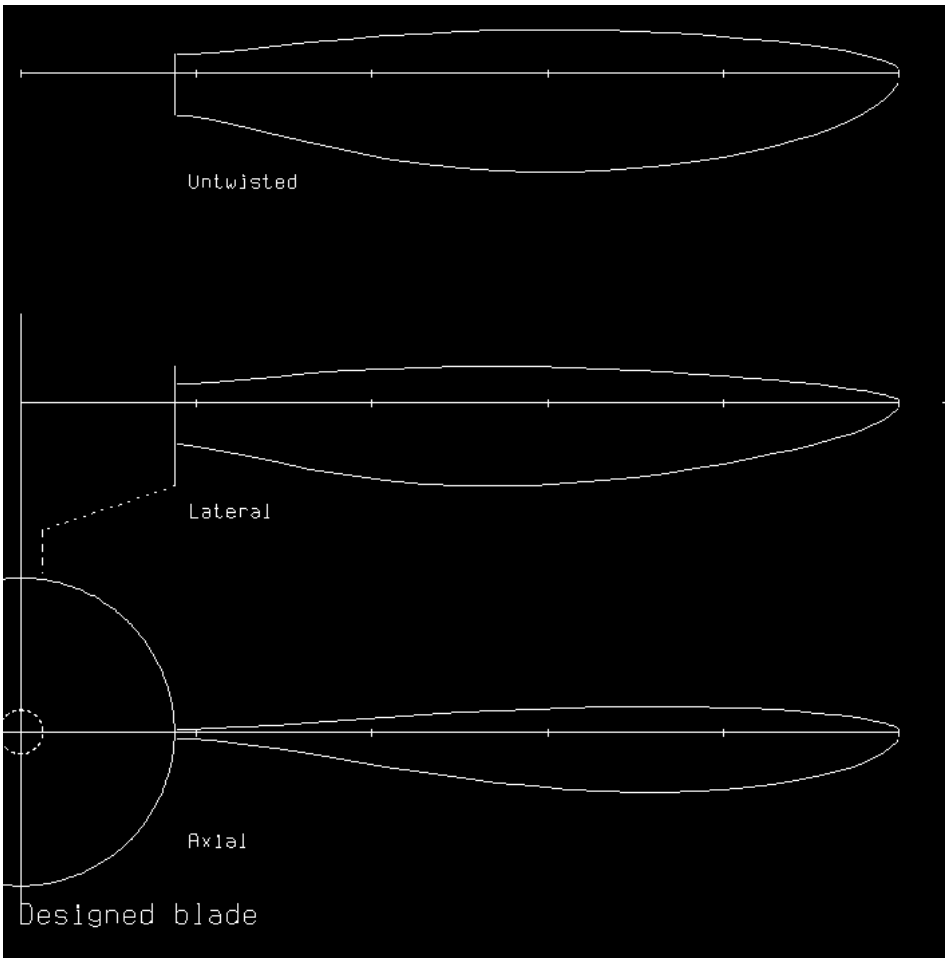

Figure 20: Rotor Profile Taken from XROTOR

XII. Structures

XII.A Material Selection

The affordability requirement is the main limiting factor in material selection coupled with the 25-year service life requirement. The availability of materials, ease of manufacturing and manipulation for structural geometries and unit price all contribute to the total cost of the aircraft over its lifetime. Aluminum 6061-T6 and 7075-T6 are the first choice for aerospace applications due to their light weight and corrosion resistance properties and are the two materials that were compared for selection for the primary structural material. Table 14 shows the material properties of each type of aluminum.

Table 14: Comparison of Material Properties of 6062 & 7075 Aluminum Alloys [42]

Material Property	6061	7075
Yield strength (ksi)	40	73
Modulus of Elasticity (ksi)	10,000	10,400
Thermal conductivity (BTU-in/hr-ft^2-°F)	1,160	900
Melting point (°F)	582 - 652	890 - 1175
Harness (Brinell)	95	150
Machinability	Good	Fair

At first sight 7075 may seem like the better candidate from the increased yield strength and stiffness, however it has many downsides for use in this project, namely, the cost. On average it can cost 40% more than 6061 and that is only considering flat plate. Making complex geometries increases the price due to the added energy needed to overcome the stronger material. Additionally, 7075 is more prone to fracturing and welding can cause it to lose the T6 heat treatment rating weakening joints. The added ductility of 6061 may also make it better suited for austere airfields by better absorbing vibration. Since 6061 is less expensive and capable of meeting the structural requirements of the aircraft, shown in the next section, it was chosen over 7075 and will be used for the wing structural analysis.

XII.B Wing Structural Analysis

The general structural design is four spars with two runners for lateral stiffness, shown in Figure 21. The runners and the spars have holes cutout for lighter construction except the rear runner in order to have a more solid structure for mounting the control surfaces. The spars and runners are 2.6 mm or approximately 1/10th of an inch, which was determined by matching the weight estimation from FLOPS compared to the weight given by SolidWorks then optimizing for strength and reduction in weight.

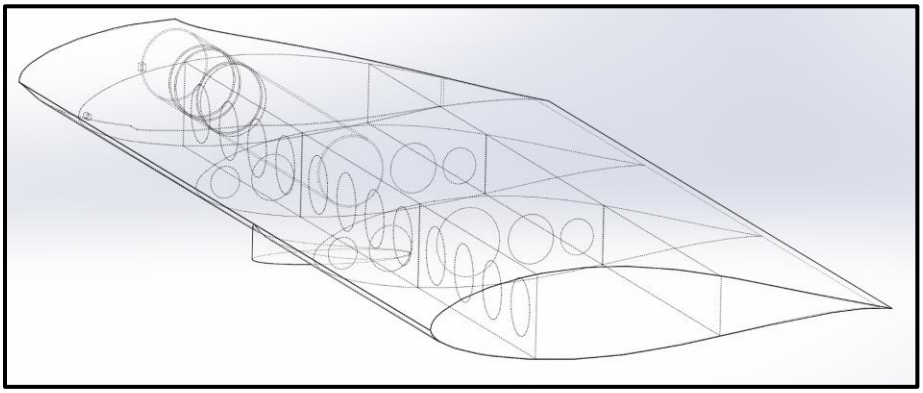

Figure 21: Wing Internal Structure

Part of the internal structure that was also important to model for the stress analysis was the connecting wing shaft, colored blue in Figure 22, that acts as the pivot for tilting and therefore the load bearing structure.

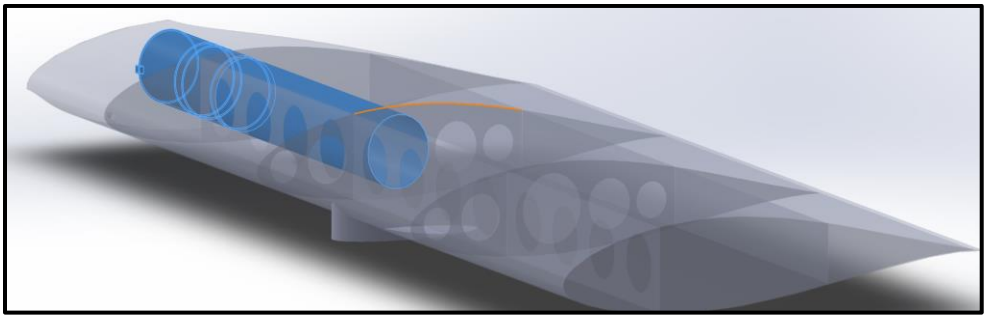

Figure 22: Internal Structure with Connecting Shaft

Structural analysis was completed using SolidWorks and with gravity set to +4g and -1g to meet the envelope of a light attack aircraft. Since the model does not have the engine or fuel included, the mass of the wing was artificially adjusted to account for those masses as if the vehicle was fully loaded.

The result of the analysis, shown in Figure 23 for the +4g case, and Figure 24 for the -1g case, were 22.1 ksi and 25.6 ksi resulting in a factor of safety of 1.8 and 1.6, respectively.

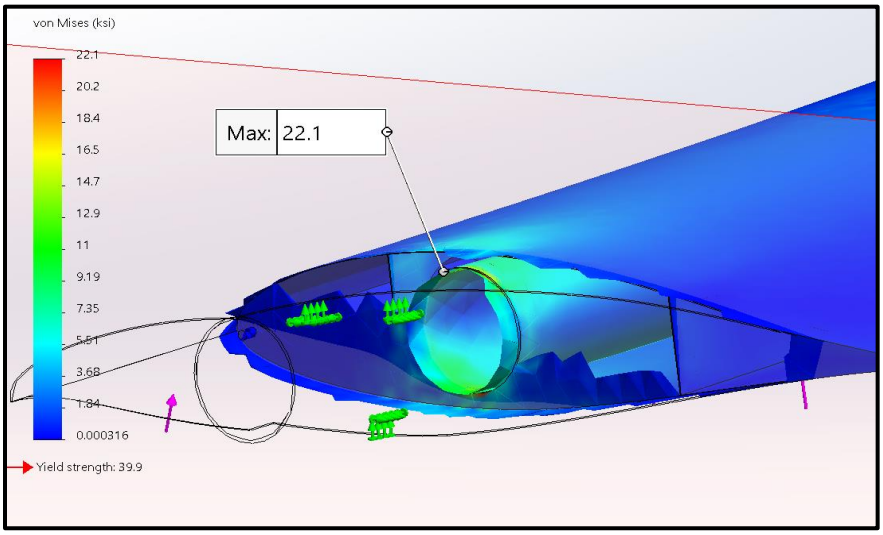

Figure 23: and Static Stress Analysis (+4g)

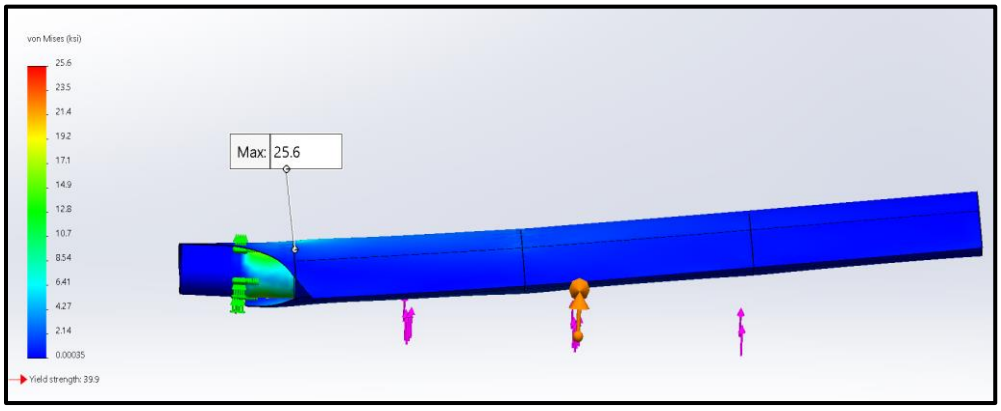

Figure 24: Static Stress Analysis (-1g)

Next, for the fatigue and life cycle analysis, three more static stress analyses were made to represent the different stresses through a flight. The simulation cycled through these states, listed in Table 15 to determine the lifespan of the wings, which will inform the lifespan of the aircraft since the wings oscillate through the most stress on the aircraft.

Table 15: Stress

Study name	Description
Static before takeoff	Full aircraft weight on ground
Static 3 after takeoff	Force of pressure on wings plus weight
Static +4g	+4g with max weight
Static -1g	-1g with max weight
Static 3 landing	On the ground minus fuel weight

These flight conditions were used for every cycle as a way of representing an above average stress amplitude since most flights would have no high g maneuvers and some would have multiple. In order to run the fatigue simulation in SolidWorks, the S-N curve, see Figure 25, needed to be input manually using data from a 2014 fatigue analysis on aluminum 6061-T6 [43]. The simulation ran for 10,000 cycles as an estimate for the 25-year life cycle requirement. 10,000 cycles would be the equivalent of one flight per day every day for 25 years.

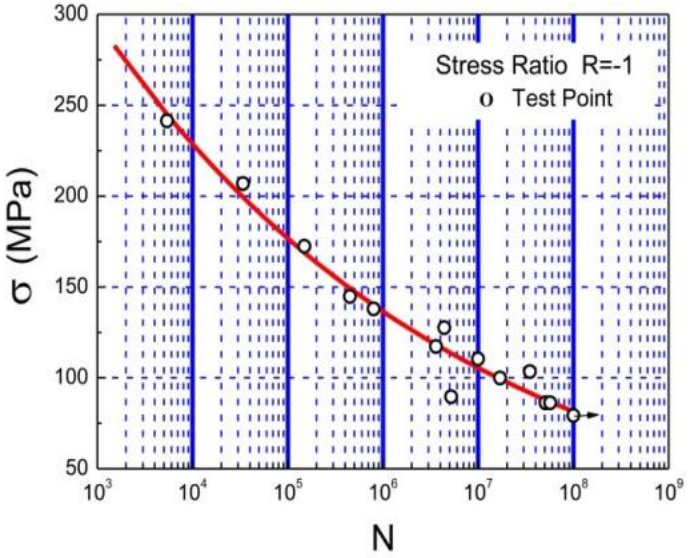

Figure 25: S-N Curve of 6061-T6 Aluminum Alloy

The result was 6.4% damage after 10,000 cycles, seen in Figure 26, and minimum full life result of 155,000 cycles, seen in Figure 27.

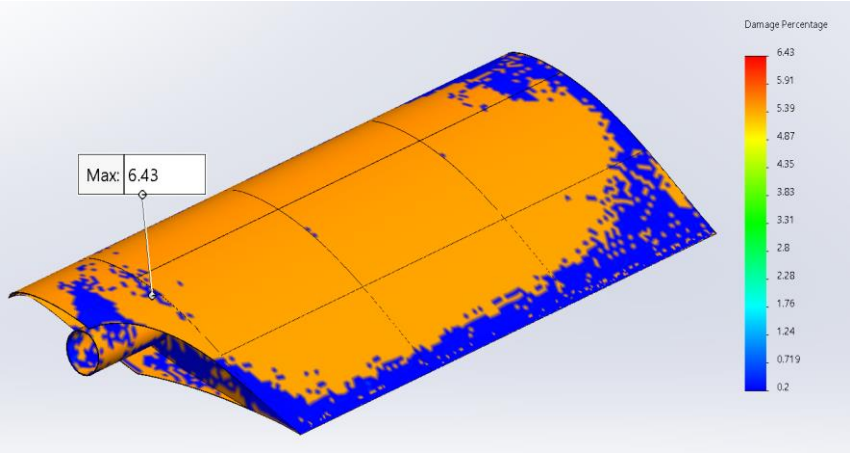

Figure 26: 10,000 Cycles

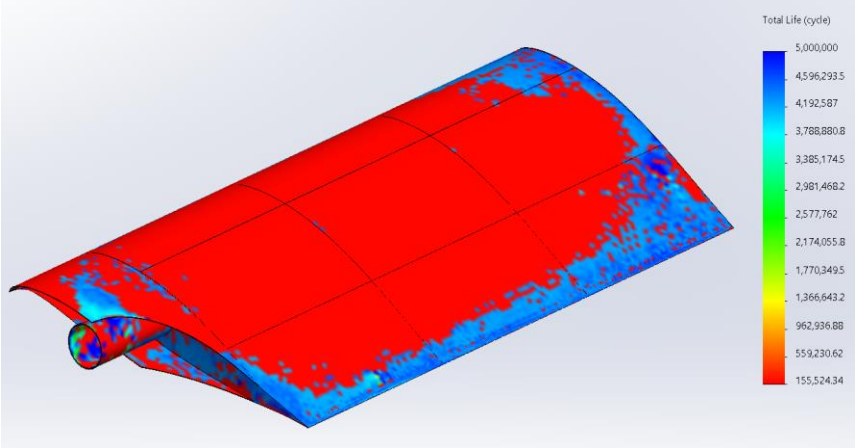

Figure 27: Full Life Cycle

These results give confidence that the structural design and material can meet the 25-year service life requirement.

XII.C Tiltwing Design

The design of the tiltwing is a balance between cost and capability. In order to keep the costs manageable, the general geometries are kept simple enough for easier manufacturing. The large thickness to chord ratio adds to the strength of the wing and provides maximum space for fuel. The wing can rotate from 0 to 100 degrees for cruise

flight and hover flight for the ferry mission, see Figure 28 and Figure 29, which shows 0 and 45 degrees respectively. This range of rotation was selected to match the CL-84's range since it is a proven design and allows for forward and backward control in the hover.

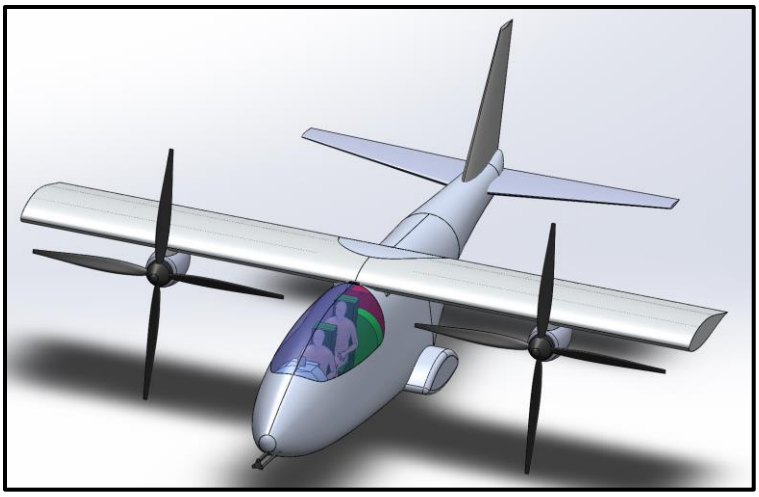

Figure 28: Showing the Wings at 0°

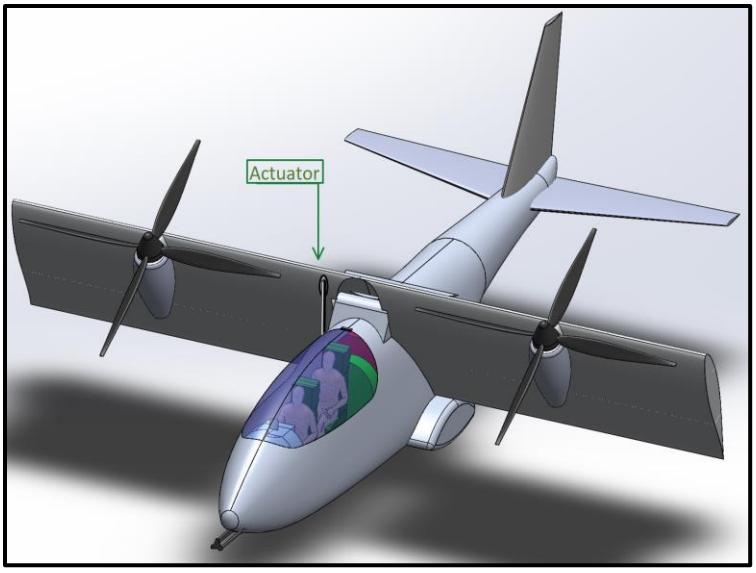

Figure 29: Showing the Wings at 45°

Additional strength will be added by having a tube through the wing pivot point to the engines which will be attached mid-wing. This also creates a protected channel for the engine connecting shaft, which is a necessary safety feature to deliver power across the wing in the event of an engine out during hover.

The material for the connecting tubular shaft and emergency drive train will need to be steel, whose weight is accounted for in the SolidWorks model. The additional strength to the wings from the steel tube insert will aid in

support of the forces in high g maneuvers helping to reduce the wear from cyclical loading of the wings. The emergency power train shaft would also be steel to handle the near instantaneous torque load when in an emergency situation.

The actuator will be placed towards the leading edge of the wing mounted to a spar near the side of the fuselage. The actuator will be a hydraulic screw and ball assembly weighing less than 30 lbs depending on the manufacturer. The worst-case scenario of there being very little fuel in the wings to counterbalance the weight of the propellers and engines would require the actuator to be able to move 1,600 lbs.

Wing design for hover control would allow for a tilt angle, like the CL-84, from 0 to 110 degrees allowing for forward and backwards control. Yaw is achieved by varying the propeller speeds inducing gyroscopic precession, however, this would be slow, so better control can be achieved by flying slowly forward and utilizing the rudder. Changing the blade angle can negate the rolling moment and tilting it to 110 degrees to halt the forward motion on a hovered landing. Roll control can also be achieved by manipulating the blade angles. To control pitch, the CL-84 utilized a tail rotor. For this design, a geared flap will provide this ability instead, negating the need for blades with a cyclic.

XII.D Fuselage

The primary concern with the fuselage is packaging all the necessary components in the aircraft. The tiltwing configuration and the desire for a reduced radar cross section resulted in the design having an internal bomb bay. Ensuring that the 3,000 lbs of armament could fit while allowing for flexibility in choice of load out is a unique challenge that is achieved by the design of the fuselage.

Ensuring that all the required flight equipment could fit, an initial packaging was done utilizing boxes to represent the avionics, see Figure 30. This is considered a worst-case scenario representation of the avionics and payload in order to determine if the fuselage design had the volumetric space to house all the components.

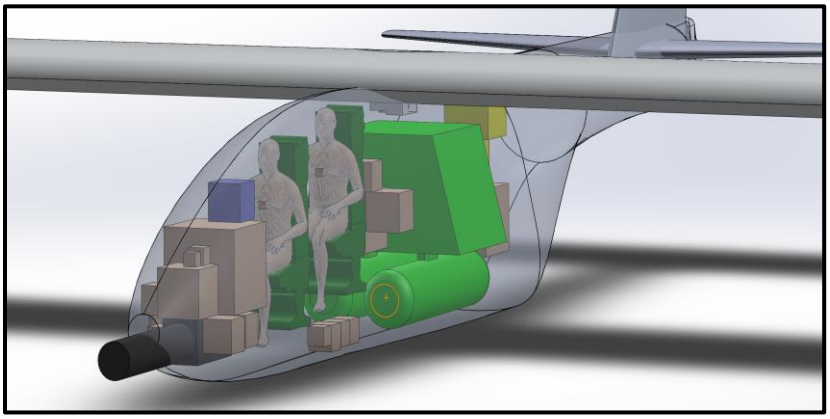

Figure 30: Worst-Case Scenario for Packaging

A new model with the final conceptual design was made with a form fitting avionics suite that accounted for the mass and volume of the required components, see Figure 31. Additionally, the rear landing gears were affixed to the outside due to space constraints around the bomb bay, so external pods were added to the fuselage to house them.

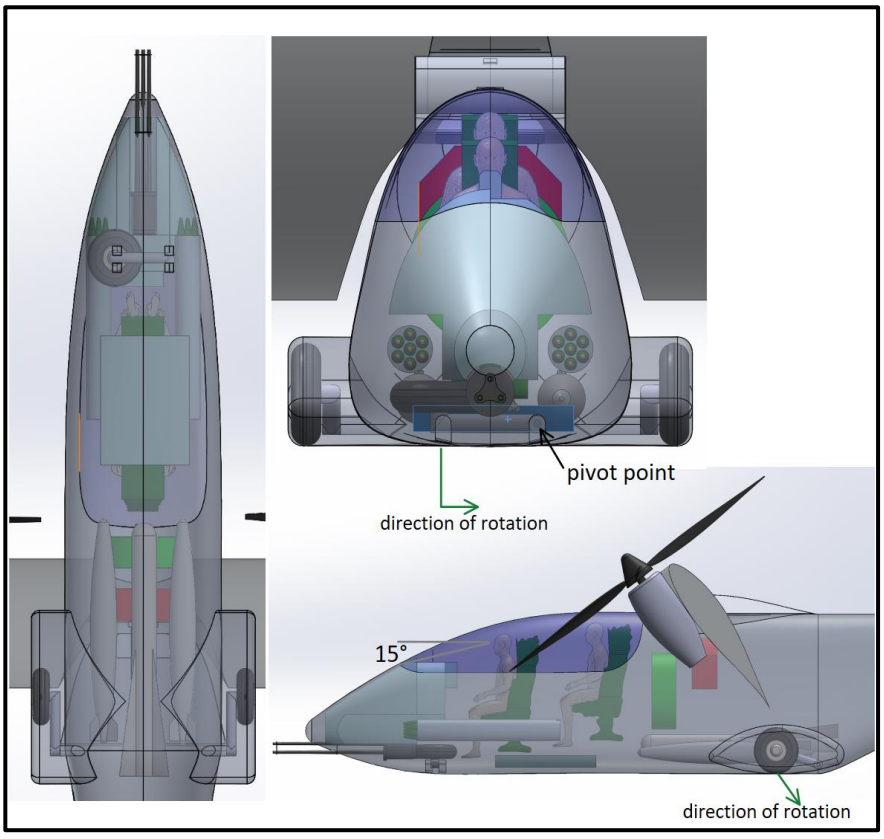

Figure 31: Final Design Fuselage Packaging

The front landing gear rotates perpendicular to the direction of travel and the rear landing gear rotates opposite to the direction of travel. The direction of the front landing gear rotation was borrowed from the A-10 Warthog as a way to both package the landing gear around the integrated gun but also to provide structural support when landing on austere airfields, the next section has more details on the landing gear. The red tank and green container below the wing in Figure 31 represent the storage for 250 lbs of reserve fuel and 4500 rounds of 20 mm ammunition, respectively. It should also be noted that the conceptual phase of the design only accounts for the space and farther design iterations are needed to design the mechanisms for the bomb bay and for feeding ammo on tracks to the integrated gun from the ammunition storage, as well as the ability to create a path for the LAU-rockets to be fired out of the fuselage. The placement of the bombs in the bomb bay is designed so that the center of gravity shifts very little when the payload is released or if the aircraft is configured for the ferry mission.

XII.D.1 Cockpit

The cockpit was designed to have adequate space for the pilots to include head clearance from the canopy, approximately 8 in for a 6 ft tall pilot with no helmet, as well as foot clearance for pedals. From the above figure, it can also be seen that there is adequate space for the zero-zero ejection seats and no obstructions in the path of the seat in the event of an ejection. The seats modeled were the MK-10, which is the same ejection seat as the A-29. The MK-10 seats are a bit older and therefore on the above average range of size and weight. This gives future design iterations plenty of room for possible adjustments to the cockpit packaging of components. See the packaging and armaments sections for a more detailed list of the components and avionics used in this model.

XIII. Landing Gear

A tricycle landing gear was chosen because it provides a flat, stable fuselage on the ground. A quadricycle was considered, but deemed unnecessary for the Kestrel's TOGW, as it would add unnecessary weight. The landing gear is retractable to provide more efficient flight. The main landing gear retracts into external pods which reduce parasitic drag during flight. The external pods allow the wheel track to be larger, but also keep the bomb bay clear. The landing gear retracts forward, which places the force of landing to be applied to the landing gear's structure instead of the retracting mechanism. This extends the life of the retracting mechanism. For the same reason, the auxiliary landing gear turns 90 degrees before retracting into the fuselage.

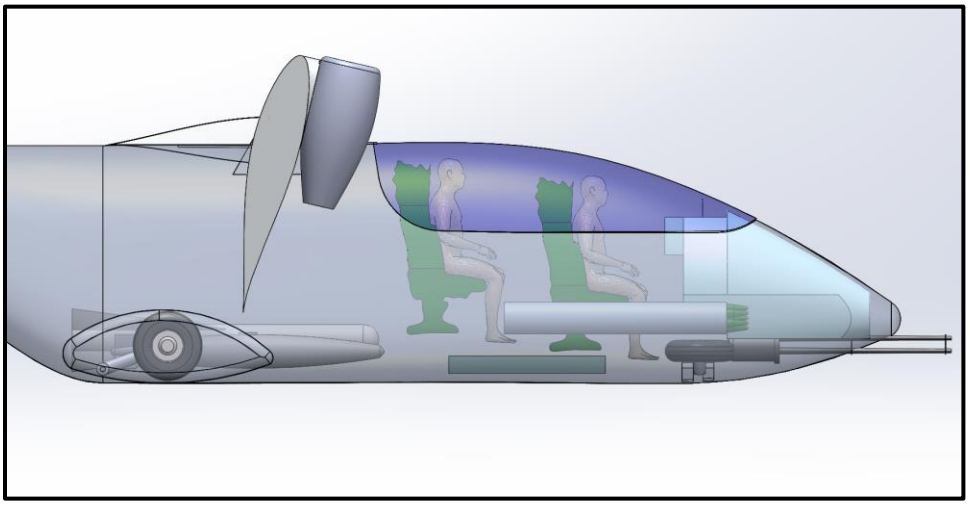

Figure 32: Landing Gear Retracted into Fuselage

XIII.A Height, Base, Track

Next, landing gear height, wheel base, wheel track, and distance between the main gear and the aircraft center of gravity were calculated concurrently. These parameters were calculated according to Chapter 9 of *Aircraft Design: A Systems Engineering Approach (2013)* by Mohammed H. Sadraey [44]. The height of the landing gear was made as high as possible in order to provide adequate clearance given the space for the wheel track on the bottom of the fuselage. This resulted in somewhat limited angles of attack for the wing on the ground. The propeller is only above the fuselage at angles of attack above 20 degrees, so this limits the possible takeoff and landing conditions. The distance between the main gear and aircraft center of gravity, and the wheelbase were calculated by setting the main gear to carry 80% of the aircraft's weight on the ground.

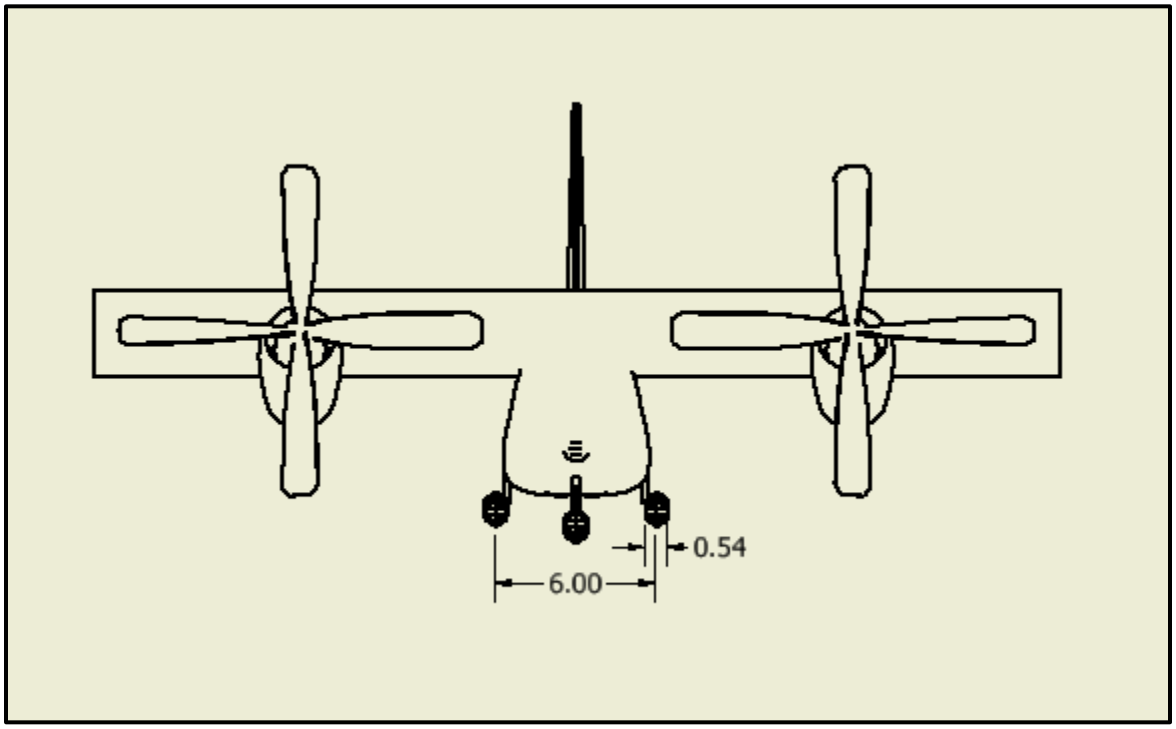

Figure 33: Landing Gear Track (ft)

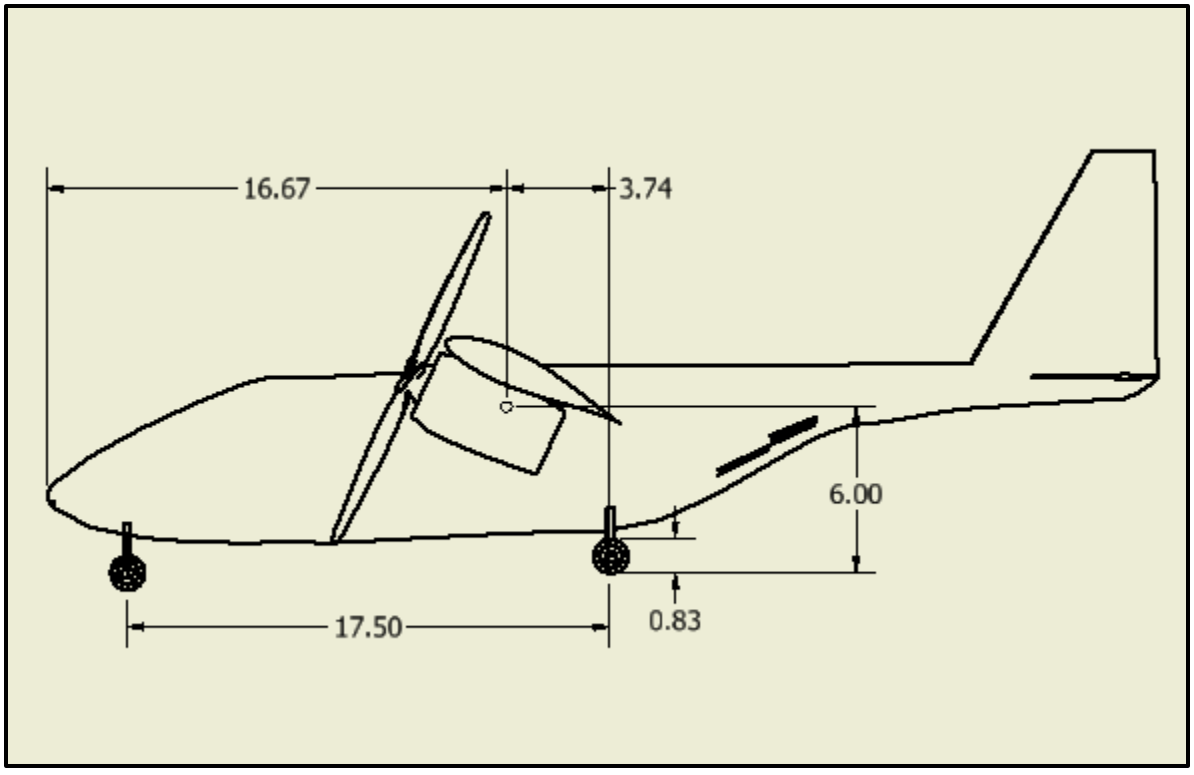

Figure 34: Landing Gear Base, Height, and Distance from C_g to Main Gear (ft)

XIII.B Tires

After calculating the position of the landing gear, tire size can finally be determined by analyzing a tire chart and finding a tire which fits the aircraft's requirements. The selected tire was the Goodyear 650G4EG1. This tire is 6.5 inches wide, 10 inches in diameter, and is rated for a load of 7738 lbs [45]. The static load on each of the Kestrel's main gear tires is 5520 lbs, so the tires are easily oversized in order to absorb additional forces experienced in taxi, take off, and landing.

XIV. Stability and Control

XIV.A Tail Design

For the aircraft's stability and control, conventional control surfaces were chosen. This decision was made with the idea of keeping the design simple while having to deal with the complications of a tiltwing. The team also found research using scale models which allowed for pitch control of a tiltwing aircraft, particularly in transitional angles of attack, using a conventional tail, a geared flap, and slats [37]. The team wanted to stay true to this design, even if high-fidelity simulations of the transitional aerodynamics cannot be performed at this point in the design process. The tail for this aircraft was initially sized using guidance from *Aircraft Design: A Conceptual Approach (1992)* by Daniel Raymer and *Airplane Design (1985)* by Jan Roskam for twin-engine turboprop aircraft [46] [47]. This sizing was refined several times in the design process in order to ensure the aircraft provided static stability, dynamic stability and controllability. The final tail size can be seen in the figures below.

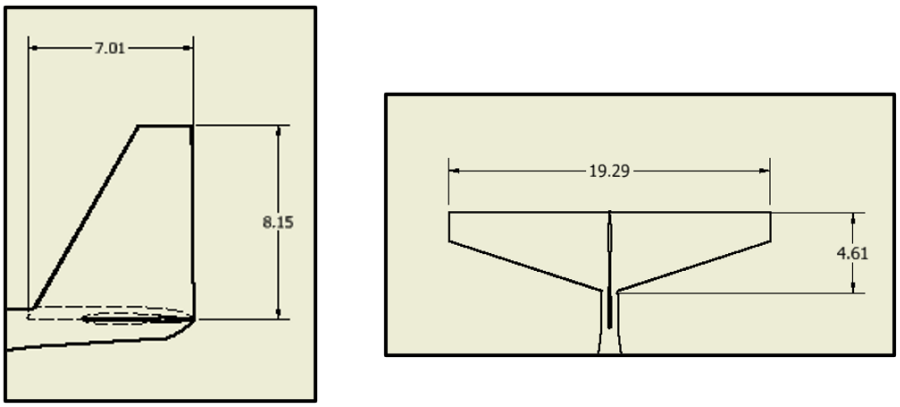

Figure 35: Tail Dimensions (ft)

Table 16: Tail Dimensions

	Horizontal Tail	Vertical Tail
Airfoil	NACA 0010	NACA 0010
Area, S (ft^2)	62	38
Volume Ratio	0.145	0.086
Aspect Ratio, AR	6	1.75
Taper Ratio	0.36	0.32
Sweep	17.5	30

XIV.B Static Stability

In order to make the aircraft sufficiently stable, static stability was verified at important flight conditions. The flight conditions were identified earlier in FLOPS and the angle of attack of the wing was adjusted in order to provide the appropriate coefficient of lift for flight. Stability of the aircraft was evaluated based on government and private industry standard stability derivatives. A VSPAero analysis was performed at each flight condition. This analysis periodically shifts aircraft parameters like angle of attack (AOA), yaw angle, roll angle, flight speed, etc. by small amounts to evaluate how quickly the aircraft returns to equilibrium. The table below shows the results at each flight condition and the stability derivatives at each condition are of the appropriate sign. The aircraft meets static stability requirements laid out by Nicolai and Carichner, as all derivatives are of the correct sign.

Table 17: Static Stability Derivatives

Segment	Mach	Alt (ft)	C_L	AOA	Cma<0	Clb<0	Cnb>0	Clp<0	CMq<0	CnBdyn>0	SM
Takeoff	0.15	1000	1.5	25	-1.103	-0.084	0.078	-0.263	-19.6	0.126	35.4%
Design Cruise	0.50	10000	0.20	0.0	-1.695	-0.072	0.162	-0.411	-24.4	0.162	34.8%
Loiter	0.27	3000	0.53	5.5	-0.837	-0.074	0.274	-0.409	-15.6	0.283	19.2%
Ferry Cruise	0.39	18000	0.37	2.5	-0.401	-0.125	0.271	-0.415	-22.9	0.277	9.3%

XIV.C Controllability

The aircraft's control surfaces were sized using the processes in Sadraey Chapter 12 [44]. These steps were followed closely, but occasionally stability parameters found using calculations or previous aircraft in the text were replaced with analysis from VSPAero. Each control surface was designed using max control surface deflection, control surface geometry, the Kestrel's geometry, and the Kestrel's stability parameters.

XIV.C.1 Aileron

The aileron is sized for roll control. Roll was characterized by a time to achieve a bank angle at takeoff conditions. The Kestrel was identified to be a Class II aircraft with a land-based runway. Sadraey stated Phase B to be the most critical design condition, so 1.9 seconds to achieve a bank angle of 45 degrees was used as the design requirement. The size of the aileron was iterated until the aircraft fulfilled the bank angle requirement. The Kestrel's aileron is large due to the low aspect ratio wing, which provides a poor lever arm for roll control.

Table 18: Roll Control Requirements - Level 1, Phase B is Analyzed [43]

(b) Time to achieve a specified bank angle change for Class II				
Level	Runway	Flight phase category		
		A	B	C
		Time to achieve a bank angle of 45° (s)	Time to achieve a bank angle of 45° (s)	Time to achieve a bank angle of 30° (s)
1	Land-based	1.4	1.9	1.8
	Carrier-based	1.4	1.9	2.5
2	Land-based	1.9	2.8	3.6
	Carrier-based	1.9	2.8	–
3	Land-based	2.8	3.8	–
	Carrier-based	2.8	3.8	–

Table 19: Aileron Dimensions

Aileron			
bai/b	**bao/b**	**Ca/C**	**da_max (deg)**
0.50	0.975	0.30	25

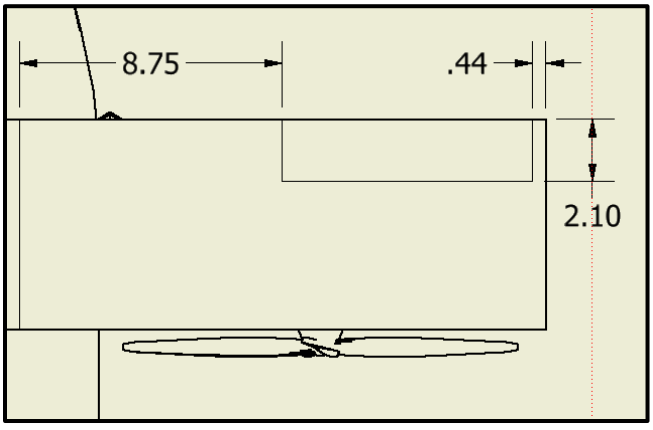

Figure 36: Aileron Dimensions (ft)

XIV.C.2 Elevator

The elevator is sized for pitch control. It was designed around two requirements: takeoff rotation and trim flight. Due to the tiltwing design, it was decided that the most reasonable takeoff rotation is 0 degrees. Trim flight requires that the elevator can be deflected for the aircraft to fly straight, level, and unaccelerated. The trim flight requirement was evaluated at the four important flight conditions. The elevator size was iteratively solved for using the process in Sadraey.

Next, the decision was made for the elevator to be significantly larger than required for both of these requirements. This was completed in order to ensure that the aircraft can have trim flight in conditions not analyzed for explicitly, but also to provide more control for the aircraft when transitioning from operating as a conventional plane to a VTOL/hover aircraft.

Table 20: Flight Conditions for Trim Flight

Segment	Mach	Alt (ft)	C_L	AOA
Takeoff	0.15	1000	1.5	25
Design Cruise	0.50	10000	0.20	0.0
Loiter	0.27	3000	0.53	5.5
Ferry Cruise	0.39	18000	0.37	2.5

Table 21: Elevator Dimensions

Elevator		
be/bh	**ce/ch**	**de_max (deg)**
1.0	0.25	25

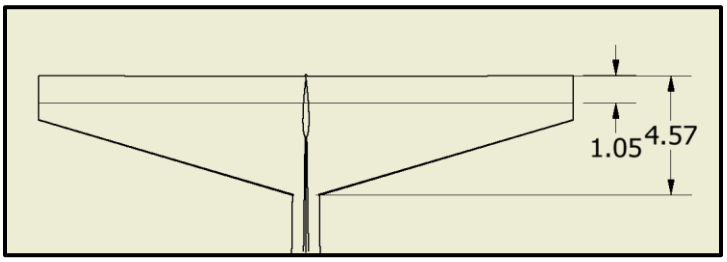

Figure 37: Elevator Dimensions (ft)

XIV.C.3 Rudder

The two main rudder design conditions are asymmetric thrust from one engine inoperable flight and a $0.2*V_{stall}$ crosswind takeoff, where V_{stall} is the stall velocity. In the event of an engine failure, the Kestrel is designed to distribute the working engine's thrust to both propellers. Due to this, the $0.2*V_{stall}$ crosswind was used as the design requirement. The process in Sadraey was used to calculate the required rudder size based on this requirement. This requirement proved difficult to fulfill and the aft part of the fuselage also had to be changed in order to have stability and controllability in yaw.

Table 22: Rudder Dimensions

Rudder		
br/bv	**cr/cv**	**dr_max (deg)**
1.0	0.25	30

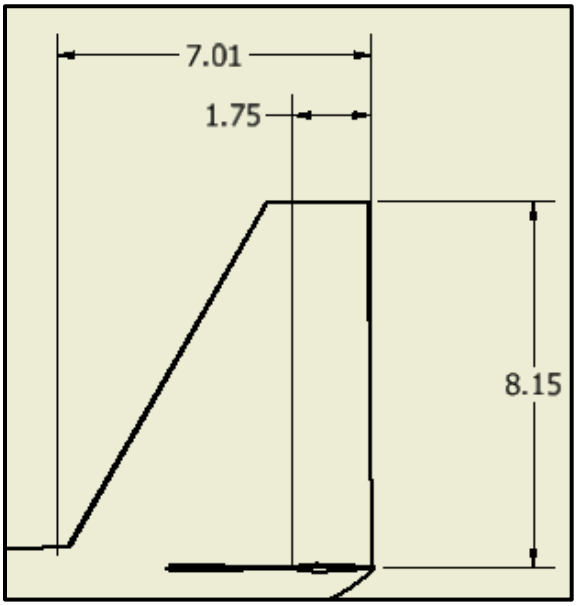

Figure 38: Rudder Dimensions (ft)

XV. Performance

XV.A Takeoff and Landing Analysis

The Kestrel is capable of vertical takeoff and landing (VTOL) at 60% payload capacity and effectively has takeoff and landing distances of 0 ft for the ferry mission. This is supported by the thrust requirements for VTOL and hover in engine sizing as well as a thrust to weight ratio, T/W, of 1.04 for the ferry mission computed within FLOPS using an engine deck for the GE T700/rotor system. The Kestrel has a T/W of only 0.908 at 100% payload capacity and is believed to be not capable of VTOL for the design mission. Thus, a short takeoff and landing (STOL) analysis was performed to accurately assess the Kestrel's ability to meet RFP requirements for the design mission.

The design must be capable of taking off and landing within 4000 ft over a 50 ft obstacle in austere conditions up at elevations up to 6,000 ft in altitude. Thus, the air density at 6,000 ft was used in all calculations for takeoff and landing to provide conservative estimates. The takeoff field length (TOFL) or takeoff distance was identified as the sum of four stages: the ground distance (S_G), rotation distance (S_R), transition distance (S_{TR}), and the climb distance (S_{CL}). These stages for takeoff are shown in Figure 39 and were computed using the methods outlined in Nicolai and Carichner Chapter 10 [18]. It was assumed that the aircraft accelerates to a takeoff velocity $V_{TO} = 1.2*V_{stall}$ before leaving the ground and transitioning from horizontal to climbing flight.

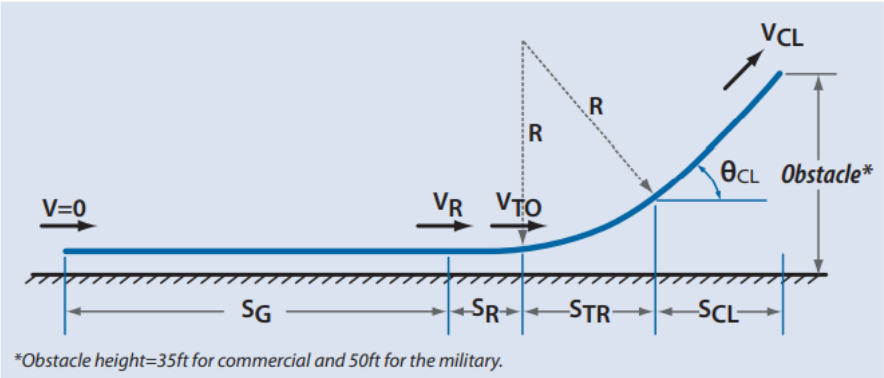

Figure 39: Breakdown of Takeoff Stages [18]

The landing field length (LFL) or landing distance was identified as the sum of three stages: the air distance (S_A), the free-roll distance (S_{FR}), and the braking distance (S_B). These stages for landing are shown in Figure 40 and were also computed using the methods outlined in Nicolai and Carichner Chapter 10. It was assumed that the

velocity over the 50 ft obstacle $V_{50} = 1.3*V_S$ and that the touchdown velocity was $V_{TD} = 1.15*V_S$, where V_S is the stall velocity for the aircraft in its landing configuration. The aircraft weight for landing was assumed to be the aircraft weight with ½ fuel remaining.

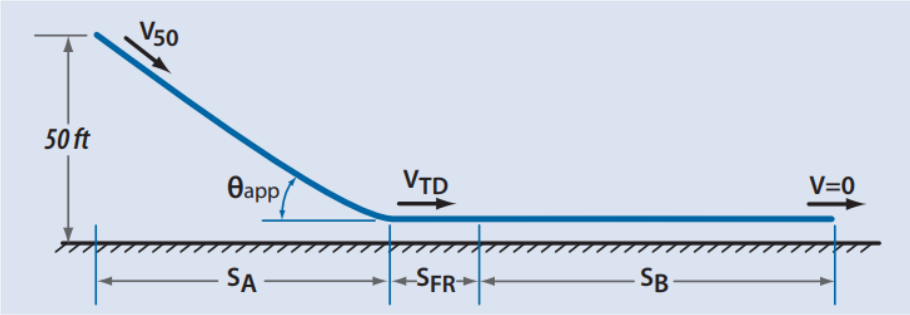

Figure 40: Breakdown of Landing Stages [18]

The effective weight and thrust of the aircraft when tilting the wing was approximated using Equations 7 and 8, where θ_T is the wing tilt angle relative to the horizontal.

$$Weff = W - Tsin(\theta_T) \tag{7}$$

$$Teff = Tcos(\theta_T) \tag{8}$$

The coefficients of lift and drag were computed as functions of the wing tilt angle using the methods outlined in Aerodynamics of V/STOL Flight by McCormick in combination with aerodynamic data from VSPAero [38]. Flap and landing gear drag coefficients were approximated using Nicolai and Carichner. The flap angle was assumed to be constant at 15 and 30 degrees for takeoff and landing respectively. The RFP specifically categorizes austere field performance as taking off and landing from semi-prepared runways such as grass or dirt surfaces with a California Bearing Ratio (CBR) of 5. The coefficients of frictions corresponding to brakes off for takeoff and brakes fully applied for landing can be seen comparatively in Table 23 for grass and dirt surfaces as outlined in Nicolai and Carichner.

Table 23: Coefficients of Frictions for Grass and Dirt Surfaces [18]

Type of Surface	Brakes Off, Average Ground Resistance Coefficient	Brakes Fully Applied, Average Wheel-Braking Coefficient
Firm and dry dirt	0.04	0.3
Wet grass	0.1	0.2

All of the above-mentioned methods and analysis were compiled into a MATLAB code to assess austere field takeoff and landing performance for the Kestrel. Takeoff distance can be seen plotted as a function of wing tilt angle for both dirt and grass surfaces in Figure 41. The Kestrel can take off within 709 ft on a dirt surface and 711 ft on a grass surface at an altitude of 6000 ft by adjusting the wing angle to 48 degrees, assuming a flap angle of 15 degrees.

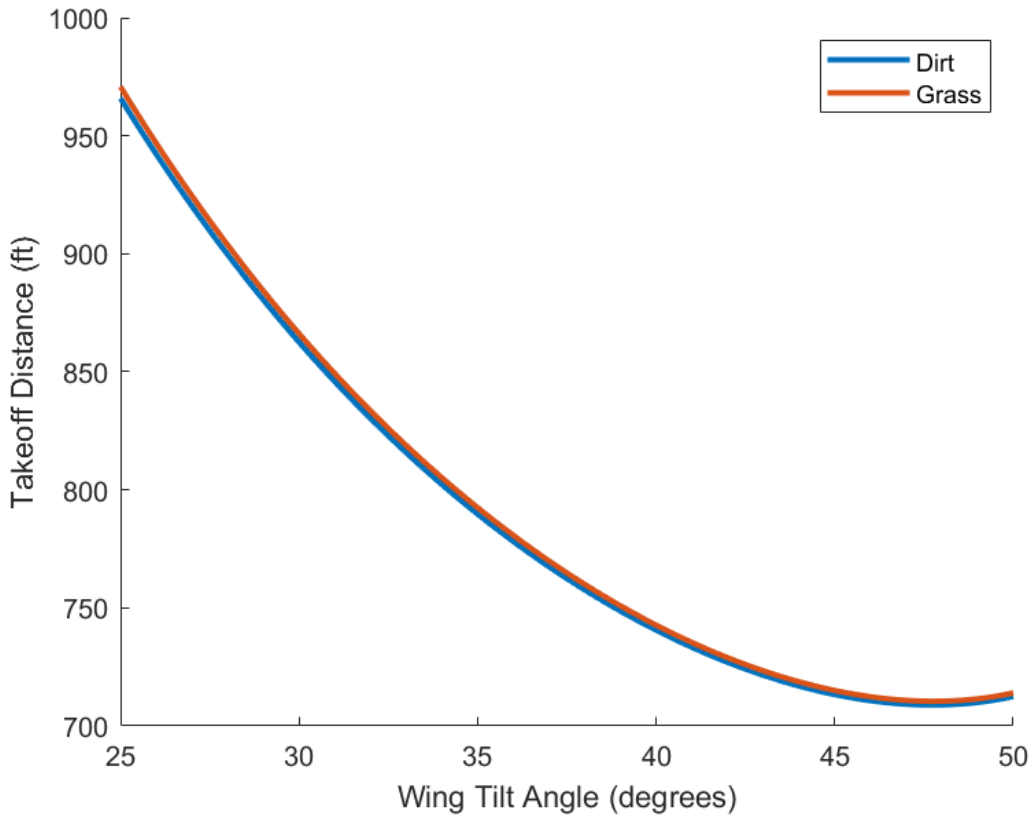

Figure 41: Short Takeoff Performance

Landing distance can be seen plotted as a function of wing tilt angle for both dirt and grass surfaces in Figure 42. The Kestrel can land within 496 ft on a dirt surface and 566 ft on a grass surface at an altitude of 6000 ft by adjusting the wing angle to 50 degrees, assuming a flap angle of 30 degrees.

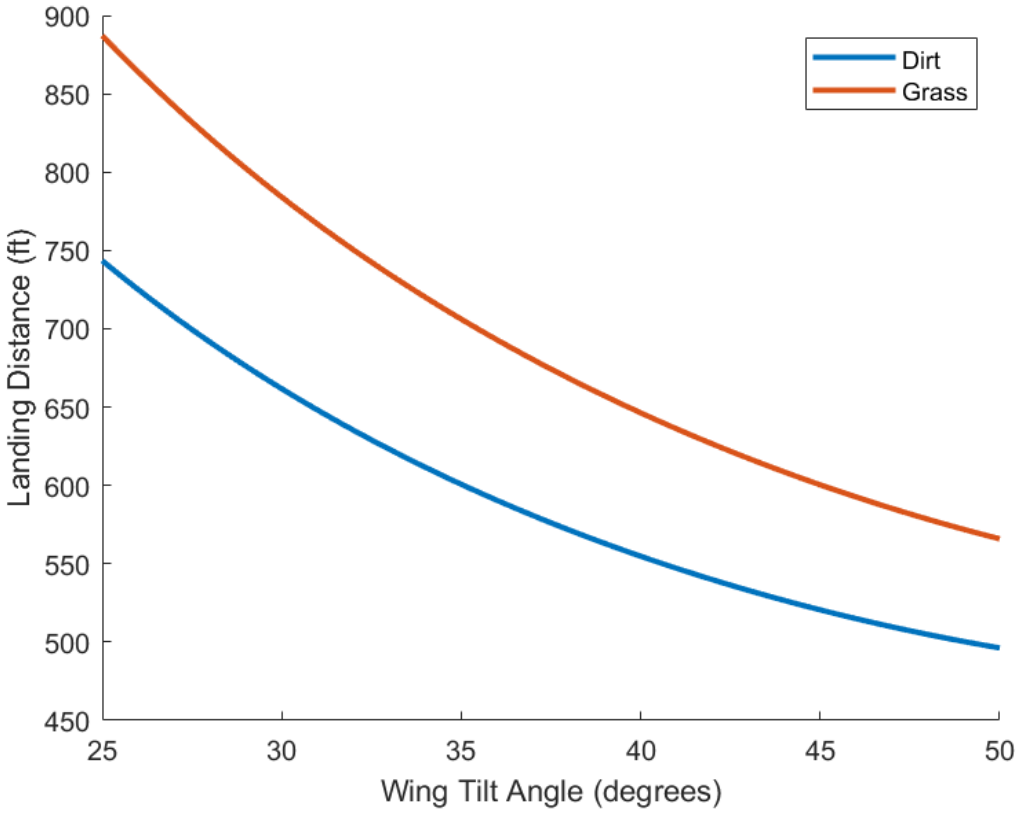

Figure 42: Short Landing Performance

The Kestrel exceeds the takeoff and landing requirements in the RFP by a significant margin for the design and ferry mission. With the ability to take off and land in less than 1000 ft at full payload capacity, the Kestrel will be able to utilize a great variety of austere airfields and terrains. VTOL capability for the ferry mission will make the Kestrel very flexible and adaptable to any situation when traveling long distances.

XV.B Mission Analysis

The Kestrel is fully capable of performing the design mission outlined in the RFP with the full payload requirement of 3000 lbs. The fuel, time, distance, Mach number, and altitudes for each segment of the design mission in full can be seen in Table 24.

Table 24: Design Mission Summary

Segment	Initial Weight	Fuel (lb)		Time (min)		Distance (nm)		Mach Number		Altitude	
		Segment	Total	Segment	Total	Segment	Total	Start	End	Start	End
Taxi Out Take Off	14169	9	9	5.0	5.0	-	-	-	0.30	-	-
Climb	14160	49	58	2.3	7.3	8.8	8.8	0.30	0.50	-	10000
Cruise	14111	179	237	18.8	26.1	100.0	108.8	0.50	0.50	10000	10000
Descent	13932	-	237	-	26.1	-	108.8	0.50	0.27	10000	3000
Hold	13932	1314	1551	240.0	266.1	-	108.8	0.27	0.27	3000	3000
Climb	12618	34	1585	1.6	267.7	6.3	115.0	0.27	0.50	3000	10000
Cruise	12584	188	1773	20.3	288.1	108.2	223.2	0.50	0.50	10000	10000
Descent	12396	13	1786	7.5	295.6	26.8	250.0	0.50	0.30	10000	-
Reserves	12384	228	2013	-	295.6	-	-	-	-	-	-
Landing Taxi In	12156	9	2022	5.0	300.6	-	-	-	-	-	-

Mission analysis was computed using NASA FLOPS. The hold segment signifies the loiter on station for four hours with no stores drops. Within FLOPS, the hold schedule definition was optimized to use the optimum Mach number for maximum endurance or minimum fuel flow to reduce consumption and weight as much as possible. The descent segment before hold was given no range credit and omitted from the FLOPS input file due to recommendations from the FLOPS user guide to omit any military beam down descents before a free segment. Including the descent segment before hold resulted in errors with FLOPS output. According to the FLOPS analysis, the Kestrel does complete the first descent within 20 minutes of the initial climb as required by the RFP. The reserves are sufficient for climb to 3,000 ft and loiter for 45 minutes. Reserve fuel was calculated using the initial climb schedule and hold schedule for loiter that minimizes fuel flow. The Kestrel is also capable of completing the ferry mission outlined in the RFP as depicted in Table 25.

Table 25: Ferry Mission Summary

Segment	Initial Weight	Fuel (lb)		Time (min)		Distance (nm)		Mach Number		Altitude	
		Segment	Total	Segment	Total	Segment	Total	Start	End	Start	End
Taxi Out Take Off	12409	9	9	5.0	5.0	-	-	-	0.30	-	-
Climb	12399	63	72	3.3	8.3	12.5	12.5	0.30	0.43	-	18000
Cruise	12336	1156	1228	213.0	221.3	897.4	909.9	0.43	0.39	18000	18000
Descent	11180	18	1246	11.5	232.8	40.1	950.0	0.39	0.30	18000	-
Reserves	11162	206	1453	-	232.8	-	-	-	-	-	-
Landing Taxi In	10956	9	1462	5.0	237.8	-	-	-	-	-	-

The cruise segment was optimized in FLOPS for the optimum Mach number for the intended range at 18,000 ft. The reserve fuel was again calculated with the same schedule definitions as the design mission and is sufficient for climb to 3,000 ft and loiter for 45 minutes. Key performance metrics for the design and ferry missions can be seen comparatively in Table 26.

Table 26: Mission Performance Comparison

Parameter	Design Mission	Ferry Mission
Design Range	250 nm	950 nm
Flight Time	290.6 min	227.8 min
Block Time	5.01 hours	3.96 hours
Block Fuel	1795 lbs	1256 lbs

The block fuel burn for the design and ferry missions is 1795 lbs and 1256 lbs, respectively. The Kestrel does have storage for 2000 lbs of fuel in the wing and thus is capable of carrying the necessary fuel for both missions. Additionally, the reserve fuel for both missions is below 250 lbs, the maximum amount of fuel within the Kestrel's reserve tank stored separately in the fuselage.

XV.C V-n Diagram

The flight envelope of the Kestrel can be seen graphically in Figure 43. The speeds were computed using cruise atmospheric conditions for the design mission at 10,000 ft and converted to knots equivalent airspeed (KEAS) to correct true airspeed for the difference in density of air at altitude compared with sea level. The design limit load factors of the aircraft were set to -1 and +4 g. Gust lines were plotted on the V-n diagram using the methods outlined in Chapter 19 of Nicolai and Carichner [18]. The aircraft's cruise speed, V_C, is 274 KEAS and maneuver speed, V_A, is 190 KEAS. The stall speed, V_S, of 95 KEAS and maximum dive speed, V_D, of 380 KEAS represent the lower and upper limits of the aircraft. The maximum dive speed represents the maximum speed before permanent structural deformation to the aircraft begins to occur and was computed using the performance constraint evaluation in FLOPS. A never exceed speed, V_{NE}, of 0.9*V_D or 342 KEAS was set to be the maximum operational speed of the aircraft to create a factor of safety. Because the Kestrel is a small, light aircraft that is significantly affected by gust loads, the never exceed speed also ensures that the dive speed gust line stays within the boundaries of the flight envelope.

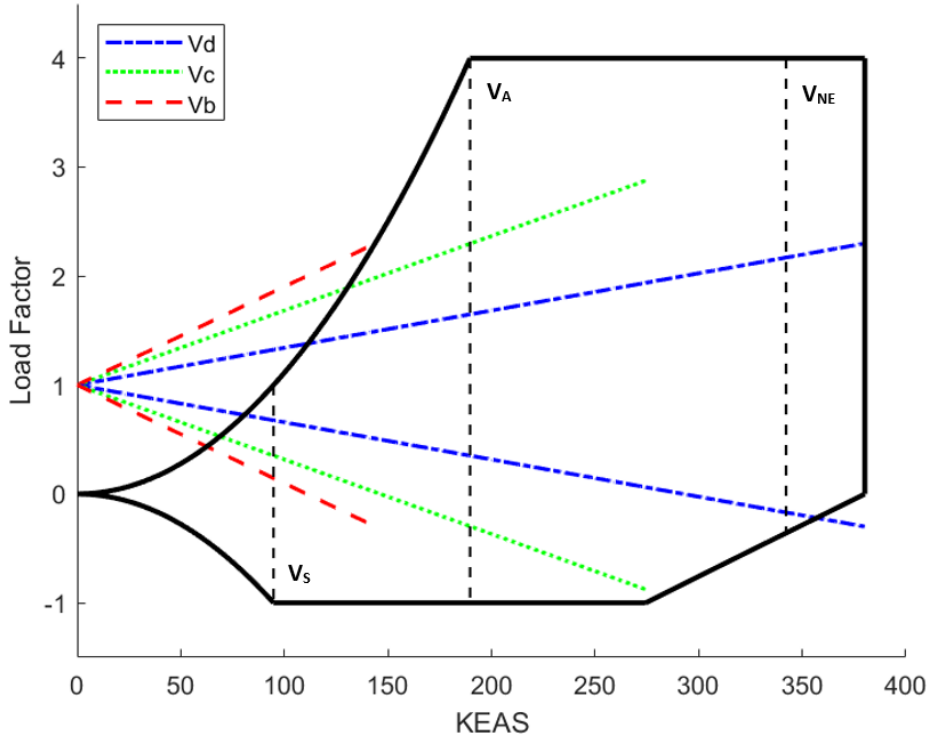

Figure 43: V-n Diagram

XV.D Payload-Range

A payload range diagram for the Kestrel is shown in Figure 44. This diagram depicts three major points of interest that describe the capability of the Kestrel. It can carry the full payload requirement of 3000 lbs for a mission radius of 250 nm which encompasses the two cruise segments of 100 nm for the design mission. At 60% of the payload requirement or 1800 lbs of armament, the Kestrel has a range of 950 nm that encompasses the cruise segment of 900 nm for the ferry mission. At zero payload and maximum fuel capacity, the Kestrel has a range of 1730 nm offering the capability to fly longer distances and missions if needed. This maximum range was computed by adjusting the payload and fuel using the rerun operation within FLOPS.

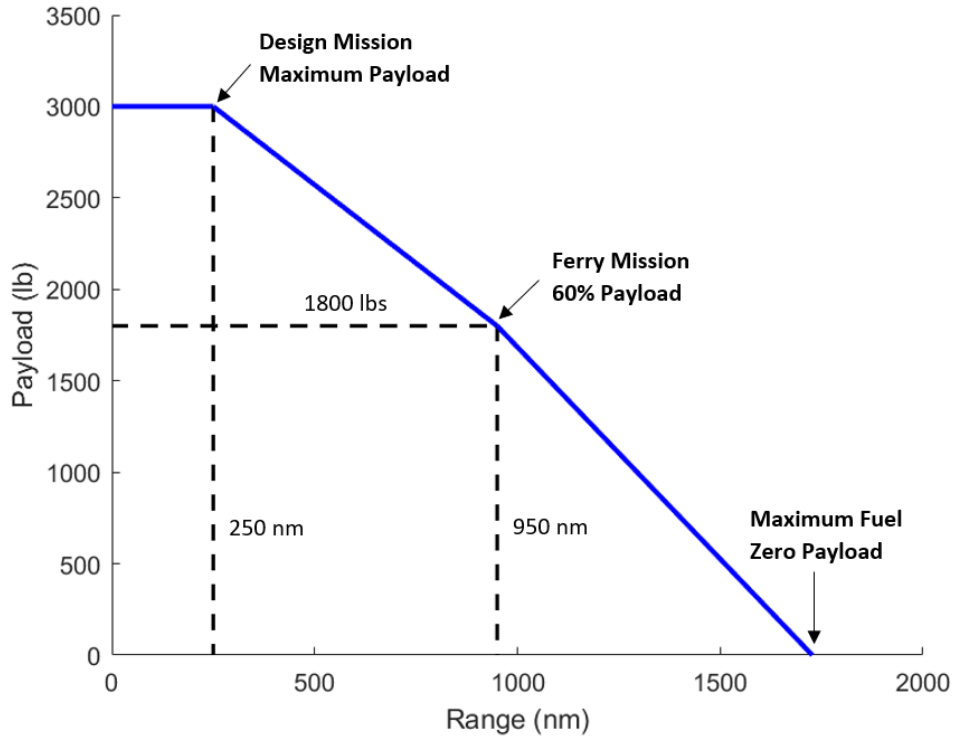

Figure 44: Payload-Range Diagram

XV.E Service Ceiling

Service ceiling is defined as the altitude at which the maximum steady state rate-of-climb potential is 100 feet per minute for a specified configuration, weight, speed and power setting according to page D-32 of JSSG-2001B [13]. In order to compute the service ceiling of the Kestrel, the minimum acceptable climb ceiling was set to 30,000 ft with a limiting rate of climb of 100 ft/min using a performance constraint evaluation in FLOPS. The Mach

number was adjusted until a maximum in the ceiling was achieved. The highest service ceiling was found at 0.63 Mach to be 38,800 ft. The Kestrel thus meets the RFP requirement of a service ceiling ≥ 30,000 ft.

XVI. Survivability

Throughout this project, survivability of the Kestrel has been a key parameter for design. The Kestrel utilizes redundancy, countermeasures, and maneuverability to keep the aircraft in flight during the missions described above. In case of an engine failure, the Kestrel uses a cross shaft incorporated into the wing structure to redirect power to the failed engine. This will allow the aircraft to disengage from the situation and make it back to the nearest possible runway. If the wing-based fuel bladders are hit, the Kestrel utilizes self-sealing bladder cells to stop major fuel loss. To compound this, reserve fuel is stored separately from the main fuel system in the fuselage in case of major damage. The Kestrel will utilize two M-130 dispensers shown in Figure 45, with one carrying 30 chaff cartridges and one carrying 30 flare cartridges. These countermeasures will be utilized in the event of a radar guided weapon or an infrared seeking missile being used against the aircraft.

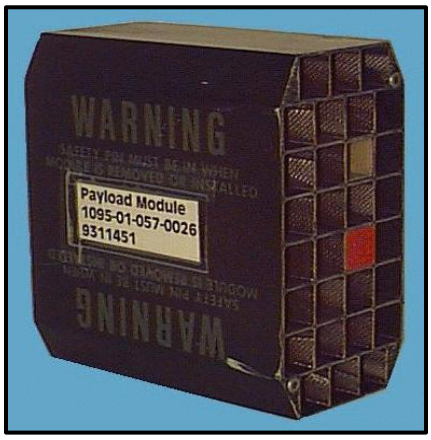

Figure 45: M-130 General Dispenser

In terms of radar and thermal signature, the Kestrel's design implements a variety of ways to reduce its signature. For radar cross section (RCS) reduction, the primary method utilized is discontinuity treatment to minimize the number of gaps and edges on the surface of the plane [48]. This design also utilizes internal bays instead of hardpoints which allows for a lower signature. Finally, the leading and trailing edge surfaces will utilize a high resistive strip to further reduce this. Cumulatively, these methods lower the amounts of sharp edges on the outside of the aircraft and allow the aircraft to have reduced radar signature. Moving on to thermal signature, the

Kestrel uses two main methods to reduce this. First, it flies subsonically, which allows the thermal signature to be greatly reduced in addition to distributing the fuel tanks along the wings and the central fuselage for use as a heat sink.

Another key aspect of survivability is the noise level of the aircraft. To effectively calculate this, XROTOR was utilized to create a ground noise footprint in decibels. As shown in Figure 46, which shows a 2D map of the noise generated by the aircraft with the plane in the middle, the sound level at the ground does not exceed 80 decibels. While not exactly silent, this shows that ground troops will not hear anything above 70 decibels or the sound level of an average vacuum cleaner until the plane is approximately 10,000 feet away, which will then become approximately 80 decibels at 5,000 feet, approximately the sound level of a garbage disposal. Keeping this noise level as low as possible keeps the airplane safe by giving hostile forces less time to react to an incoming aircraft such as the Kestrel.

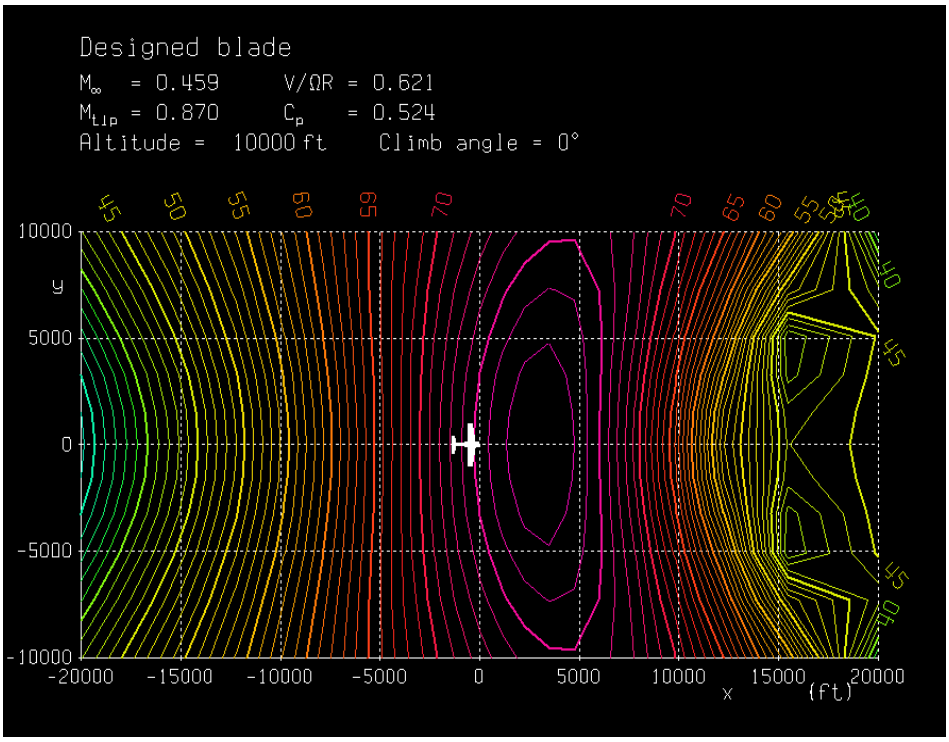

Figure 46: Sound Profile in Cruise

A crucial design study was made in terms of survivability, which is the addition of armor plating or a titanium bathtub like the A-10 Warthog has. This would provide extra defense for the pilots than what the aircraft would have with just the aluminum alloy that it is made out of. This however would add both weight and cost to the

aircraft. Knowing that a lower weight would help to achieve VTOL capability at as low a cost as possible, the decision was made to forgo armor in support of maneuverability. This permits the Kestrel to effectively maneuver at maximum speeds as spoken about in the above discussion.

XVII. Cost Analysis

XVII.A Affordability and Overview of Costing Methods

Cost analysis was used to inform the design process and to justify the aggressive tiltwing design that makes the Kestrel unique in the light attack aircraft class. Balancing affordability while maintaining the performance aspects that set the Kestrel apart from the competition was constantly taken into consideration through iterative cost models. When determining engine placement on the wing, cost was an important variable to take into consideration. After both aerodynamic and costing analysis of mid-wing engine placement versus wingtip engine placement, it was unanimously determined that the aerodynamic benefits from negating wingtip vortices was not worth the added cost required to strengthen the wing. Cost was also a driving factor in material selection and ultimately led to the use of aluminum alloy 6061 vs. 7075, despite the material advantages that aluminum alloy 7075 displayed.

For the cost analysis models developed for this project, Jan Roskam's *Airplane Design*, specifically Part VIII, served as the foundation for each cost model using Advanced Aircraft Analysis 4.0 [47] [49]. In order to achieve an accurate cost model, an initial model was created for the A-29 Super Tucano and calibrated to flyaway cost of around $12M in 2019 according to online literature [50]. The model was originally designed for purchase in the year that the literature occurred in order to achieve an accurate calibration, and it was then adjusted to 2025 dollars to reflect the timeline of Project Kestrel through a cost escalation factor that takes both past and expected future inflation into account. Program cost analysis was based off of a total of 150 aircraft manufactured, for 3 procurement lots of 50 aircraft each. This number was determined by comparison from an Air Force Light Attack Aircraft Program Request, and information about current A-29 units in service. When light attack aircraft were first requested by the Air Force, 100 aircraft were requested in 2008, and today, there are more than 200 A-29 aircraft in service [51] [52]. The number of 150 manufactured aircrafts was determined by splitting the difference to account for the additional life of the Kestrel when compared to the A-29. The life-cycle cost (LCC) for each model was determined using operating costs over the service life indicated by the RFP, which implies 600 annual flight hours

over a 25-year span to achieve 15,000 flight hours, while operating costs were calculated using 1200 annual flight hours over the course of one year, averaged over the three stated mission types: design, ferry, and training. This achieved a clearer picture of hourly operating costs without having additional factors associated with lifetime use skew the output. However, in order to display realistic LCCs, these additional factors had to be taken into account when evaluating the program as a whole, leading to the change in the input of annual flight hours and years of operation. A profit margin of 10% was selected for each military fighter aircraft, and JP-4 type fuel costing $3.06/gallon was used in analysis. A comparative table for the cost models developed throughout the process can be observed below as Table 27, and a comparative table for program operating cost elements is also featured below as Table 28.

Table 27: Comparative Aircraft Cost Analysis for the Kestrel and Relevant Competitive Aircrafts

Aircraft	Conventional		Tiltwing	
	A-29	AT-6	CL-84 (STOL/VTOL)	Kestrel (STOL/VTOL)
Year Purchased	2025	2025	2025	2025
Program RDT&E Costs	$463.1 M	$418.7 M	$621.3 M	$589.7 M
Flyaway Cost (/aircraft)	$16.84 M	$15.77 M	$21.02 M	$20.42 M
Total Operating Costs (/hour)	$3,426	$3,419	$3,954	$3,868
Program Life Cycle Cost	$10.52 B	$10.35 B	$12.23 B	$11.97 B

Table 28: Comparative Program Operating Cost Elements for the Kestrel and the A-29

Aircraft	Conventional	Tiltwing
	A-29	Kestrel
Program Cost of Fuel, Oil and Lubricants	$353.8 M	$299.7 M
Program Cost of Direct Maintenance Personnel	$2.845 B	$3.225 B
Program Cost of Consumable Materials	$411.1 M	$465.9 M
Program Cost of Depot	$710.3 M	$878.7 M
Program Cost of Spares	$631.4 M	$878.7 M

XVII.B Key Assumptions

Many analogous assumptions were made in constructing the cost models for this project and discrepancies across each different cost model followed, with results displayed in Tables 27 and 28 that represent the price disparities between different aircraft. Similar aircraft tend to have similar cost models, with weight and maximum velocity being impactful parameters causing much of the difference within the groups of conventional and tiltwing aircraft. Many of the assumptions that needed to be made for the cost models had to do with the difference in design between these two groups of aircraft. In this analysis of assumptions, the A-29 and AT-6 will often be referred to as conventional aircraft, while the CL-84 and Kestrel will be referred to as tiltwing aircraft, for grouping purposes. For RDT&E cost, complexity of design was the biggest assumption resulting in cost disparities between the conventional aircraft and tiltwing aircraft. While the CL-84 was designed in the 1960's, meaning that there is past research and data about tiltwing aircraft, it did not seem justified to assign each group the same difficulty factor that reflects design complexity. With that being said, only a 10% increase in this parameter was implemented due to the presence of relevant past data. This is a large part of the increase in RDT&E as well as flyaway cost between groups. Additional test facilities for STOL and VTOL capabilities also help account for the increase in RDT&E cost displayed in Table 27, though this is only responsible for a slight increase. Total operating costs also fluctuate greatly between the different groups, because the output took many direct and indirect factors into account. The elements representing the largest disparities between groups can be observed in Table 28. As far as efficiency in fuel burn, the Kestrel was the most efficient aircraft, followed by the AT-6, A-29, and CL-84, respectively. The complexity of the tiltwing design led to an increase in total operating cost. The cost of spares for the tiltwing design used an increase in cost of spares factor from operations of about 25%. This number was determined because of the additional engine as well as the added mechanisms responsible for tilting the wing and transferring power from one engine to another in the event of a failure. Increased aircraft size also played a role in the increase in operating costs. The tiltwing aircraft featured an approximate 12% increase in cost of depot factor for the aircraft, and this number was determined by linear approximation of cost of depot factor and aircraft area of data from known aircraft. The increase in consumable materials as well as the cost of direct maintenance personnel can be attributed to the increased maintenance man hours per flight hour for tiltwing aircraft. Because of the increased design complexity, a 13.3% increase from 15 hours/hour to 17 hours/hour was implemented. Observability factor was another assumption increasing the cost of the Kestrel relative to all other comparable aircraft. Because the Kestrel is the only aircraft to

utilize internal storage for all weapons, a 5% increase in stealth technology factor was implemented, which had a slight effect on RDT&E as well as flyaway costs.

XVII.C Results

Both Tables 27 and 28 from above will be referenced throughout the following discussion. The Kestrel, came in below the LCC of the CL-84, but above both of the conventional aircraft that were analyzed. Though many aspects of cost analysis of the Kestrel design suffered due to its increased complexity compared to conventional aircrafts, the increase in price was justified due to the performance, reliability, and supportability enhancements that the Kestrel displays. Due to literature describing the A-29 as the industry standard for light attack aircraft performance, this aircraft was the main focus of design justification in terms of performance benefits against increased cost. In terms of program LCC, the Kestrel comes in at 13.7% above that of the A-29, which is justified by the increase in multiple performance statistics. The cost analysis takes both the STOL and VTOL capabilities that the Kestrel possesses into account during the design and ferry missions, respectively. The STOL design analyzed for the design mission led to an approximate 76% reduction in TOFL versus the A-29, and an 82.4% reduction in LFL. Top speed of the aircraft came in at 6.9% above that of the A-29 [4], which is crucial for survivability of the aircraft in hostile environments. On top of this, the Kestrel is a far more reliable aircraft due to its dual-engine design. While the conventional light attack aircraft analyzed only have one source of power, the Kestrel has two, and can transfer power from one to the other in the case of a failure. The ability to house all weapons inside adds to survivability as well, which is a feature that no other aircraft that was analyzed offers. Maintainability does take a hit with the more complex tiltwing design and additional engine, and the associated cost increase is reflected in Table 28. Producibility was also negatively impacted by a complex design, with those results seen in increased RDT&E and flyaway costs.

It should be noted that the Kestrel is significantly cheaper than existing attack helicopters like the AH-64E Apache while providing much of the same capability. A 2021 fiscal year budget request by the DOD for the new build of the AH-64E in 2021 totaled $69.2 M for a quantity of two [53]. This puts the flyaway cost of the AH-64E at $34.6 M in 2021. The flyaway cost of the Kestrel in 2025 is almost 41% cheaper, without accounting for potential inflation of the AH-64E’s cost.

The results from cost analysis are not without its flaws. For starters, military costing data is scarce, which leads to assumptions based on comparative models, as well as an inability to go into great detail about supplier price of raw materials. For the comparative models of the CL-84, AT-6, and A-29, liberties had to be taken in regard to fuel burn because not enough data was available online to perform an intensive FLOPS analysis of both design and ferry missions. This led to the estimated amount of fuel burn exceeding what is possible to complete the design missions within the competition design payload requirements for the AT-6 and the A-29. With that being said, the Advanced Aircraft Analysis 4.0 costing software used is fairly low fidelity and does not allow for variation based on supplier data, regardless of its level of availability. The Roskam textbook and model also does not offer in depth information about fundamental assumptions related to cost elements. For example, avionics cost is difficult to predict for military aircraft because such a wide range is given for industry averages as a factor of the market price of the aircraft. Additionally, the engine sizing for the Kestrel was very conservative based on analogous analysis to the CL-84 for safety purposes of the design. While both the VTOL and STOL weight are slightly under that of the CL-84, the Kestrel's engines are about 25% more powerful than the CL-84's Lycoming T-53 engines, which implies that with further analysis, VTOL capabilities are likely to be possible at the design mission weight. This would only strengthen the argument that the additional cost of the Kestrel aircraft is justified by performance and supportability enhancements.

XVIII. Future Work

Because of the complexity of tiltwing aerodynamics, limited time and resources made it difficult to analyze the transition between hover and steady level flight. A quantitative assessment of acceleration and deceleration, wing stall, and control during transition would greatly improve the fidelity of the design. Wind-tunnel tests would serve as the basis for determining flow characteristics of a tiltwing aircraft with the wing at an angle in forward speed [21]. Additionally, wind-tunnel or advanced analytical methods would be used on the control surfaces of the aircraft. It is important to ensure the surfaces do not experience flow separation at their max deflection for a controllable aircraft [44]. The fuselage internal structure also would be modeled in greater detail to more accurately represent packaging and structural arrangement of the Kestrel. The CL-84 is cited as having a bonded stringer and skin frame with its cross section consisting of longeron construction [11]. Addition of such a frame would improve the level of confidence in the ability of the Kestrel to maintain its predicted service life, as well as a rigorous study

of the wear experienced by the landing gear over time in austere conditions. The use of Multidisciplinary Design Analysis and Optimization (MDAO) computer methods and algorithms could aid in convergence to a higher performing aircraft. Ideally, the wing area, chord length, fuselage diameter, rotor diameter, and a plethora of other dimensions of the aircraft could be optimized to reduce drag and maximize lift all while keeping cost to a minimum. Improving the team's understanding and familiarity with NASA FLOPS would be a potential pathway to refining the design as the software possesses some of these optimization functions for sizing. Designing a custom propulsion system would also be an area of improvement since the GE T700 engine was not specifically designed for the Kestrel. Tiltrotor aircraft are known to need modification for supporting the oil system in the engines due to venting problems that result from tilting the engine [22]. Similar modifications would need to be identified and incorporated into the Kestrel's tiltwing design. A custom gearbox would also be designed in detail to efficiently bring the engine shaft rpm to the rotor rpm.

For the structural design, a deeper analysis of the mechanisms for the bomb bay and the actuator for the tiltwing need to be conducted. The weight of the actuator was included in a general weight increase to the wing as part of the unaccounted and miscellaneous weights. Also, the stress on the actuator associated with operation in slow flight needs to be determined to assure that the associated pressure to the wing does not cause the actuator to structurally fail. Additional work on analysis of vibration while the wings are under stress would strengthen the belief that the service life will not be reduced as to not meet the RFP's requirements when consistently operating on austere airfields.

XIX. Conclusion

High-end, expensive to operate fighters like the F-15 Strike Eagle and F-16 face very little threat from enemy defenses when flying CAS missions and have reduced loitering times [54]. These in-service aircraft were also not designed to operate continuously from extremely austere runways. Thus, attack helicopters have been used to fill this gap but are limited by their service ceiling, aerodynamic disadvantages, poor survivability to small arms fire, and maintenance issues. The desire for affordable light attack aircraft began in 2009 with the Air Force's Light Attack/Armed Reconnaissance (LAAR) or Light Air Support (LAS) program and the need for such an aircraft persists to this day. The AIAA RFP describes such an aircraft and the Kestrel was designed accordingly.

The Kestrel is a tiltwing light attack aircraft that leverages the flexibility of helicopters with the survivability, range and payload of a fixed wing platform. It can carry a payload of 3000 lbs with provisions for missiles, rockets, bombs, and an integrated gun that will all be crucial in delivering supporting fire while loitering in a CAS mission within 250 nm. While operating in austere conditions at a TOGW of 14,170 lbs, takeoff distance and landing distance are as low as 708.9 ft and 496.2 ft, respectively. The Kestrel has a service ceiling of 38,800 ft and is more than capable of meeting the 25-year, 15,000 hours service life requirement due to its lightweight, yet robust design. The Kestrel offers VTOL capability for the completion of ferry missions within 950 nm when carrying 60% of its payload capacity, making the aircraft adaptable to various types of geographic regions and terrain. At a unit cost of $20.42 million, the Kestrel offers helicopter-like utility at only a small fraction of added cost relative to comparators like the AT-6 and A-29. The team is confident in the Kestrel's potential to make an impact on the battlefield in CAS while satisfying all of the requirements outlined in the RFP for a light attack aircraft.

XX. References

[1] AIAA, "Request for Proposal: Austere Field Light Attack Aircraft," 2020. https://www.aiaa.org/docs/default-source/uploadedfiles/education-and-careers/university-students/design-competitions/undergraduate-team-aircraft-design-competition/aiaa-2021-undergraduate-team-aircraft-design-rfp---light-attack-aircraft-2-.pdf?sfvrsn=b54e3cac_2

[2] DOD, Joint Publication 3-17, Air Mobility Operations, *Department of Defense*, 5 February 2019. https://fas.org/irp/doddir/dod/jp3_17.pdf

[3] Dunbar, B., "Technology Readiness Level," *NASA*, 28 October 2012. https://www.nasa.gov/directorates/heo/scan/engineering/technology/technology_readiness_level

[4] Sierra Nevada Corporation and Embraer, "A-29 Specifications," *Built for the Mission*, 2018. https://www.builtforthemission.com/a-29-super-tucano/a-29-specs/

[5] "EMB-314 Super Tucano / ALX Trainer and Light Attack Aircraft," *Airforce Technology*, 2021. https://www.airforce-technology.com/projects/super_tucano/

[6] "Embraer Super Tucano," *Aero Corner*, 2021. https://www.aircraftcompare.com/aircraft/embraer-super-tucano/

[7] "AT-6 Wolverine," *Textron Aviation Defense*, 2017. https://defense.txtav.com/-/media/beechcraft-defense/files/at6-productcard.ashx

[8] "AT-6 Wolverine Light-Attack Aircraft," *Air Force Technology*, 2021. https://www.airforce-technology.com/projects/6-wolverine-light-attack-aircraft/

[9] Horne. T. A., "AT-6 Wolverine: On the Prowl," *Aircraft Owners and Pilots Association*, 1 April 2020. https://www.aopa.org/news-and-media/all-news/2020/april/pilot/turbine-at-6-wolverine-on-the-prowl

[10] Upton, B., "Design and Development History of the Canadair CL-84 V/STOL Tilt-Wing Aircraft," *Canada Aviation Museum*, 2013. https://documents.techno-science.ca/documents/CASM-Aircrafthistories-CanadairCL-84VSTOLhistory.pdf

[11] Sullivan, T. M., "The Canadair CL-84 tilt wing design," AIAA Paper 93-3939, August 1993. https://doi.org/10.2514/6.1993-3939

[12] DOD. MIL-HDBK-516C, Department of Defense: Airworthiness Certification Criteria, 12 December 2014. http://everyspec.com/MIL-HDBK/MIL-HDBK-0500-0599/MIL-HDBK-516C_52120

[13] DOD, JSSG-2001B, Department of Defense Joint Service Specification Guide: Air Vehicle, 30 April 2004. http://everyspec.com/USAF/USAF-General/JSSG-2001B_25156/

[14] DOD, JSSG-2006, Department of Defense Joint Service Specification Guide: Aircraft Structures, 30 October 1998. http://everyspec.com/USAF/USAF-General/JSSG-2006_10206/

[15] OpenVSP, Version 3.22.0, NASA, 2020. http://openvsp.org/download.php

[16] Boechler, K., "Going Tactical: A New Strike Aircraft for the Afghan Air Force," *Small Wars Journal*, 1 October 2013. https://smallwarsjournal.com/jrnl/art/going-tactical-a-new-strike-aircraft-for-the-afghan-air-force#:~:text=The%20A%2D29%20requires%202%2C950,and%202%2C820ft%20to%20land

[17] Chana, W. F. and Sullivan T. M., "The Tilt Wing Configuration for High Speed VSTOL Aircraft," AIAA, 1994. https://www.icas.org/ICAS_ARCHIVE/ICAS1994/ICAS-94-6.3.2.pdf

[18] Nicolai, L. M., and Carichner G. E. *Fundamentals of Aircraft and Airship Design, Vol 1*, AIAA Education Series, Virginia, 2010.

[19] MATLAB, Version 9.7.0 (R2019a), The MathWorks, Inc, Massachusetts, 2019. https://www.mathworks.com/products/matlab.html

[20] Salaymeh, A., A New Conceptual Design Tool for General Aviation Aircraft (FLEX), Linköpings Universitet, 2018. https://liu.diva-portal.org/smash/get/diva2:1241559/FULLTEXT01.pdf

[21] Gallant, R., Scully, M., and Lange, W., "Analysis of VSTOL Aircraft Configurations for Short Haul Air Transportation Systems," Massachusetts Institute of Technology, Flight Transportation Laboratory, Technical Report FT-66-1, Massachusetts, 1966. https://dspace.mit.edu/bitstream/handle/1721.1/67991/FTL_R_1966_01.pdf?sequence=1&isAllowed=y

[22] Maisel, M. D., Giulianetti D. J., and Dugan, D.C., "The History of the XV-15 Tilt Rotor Research Aircraft: From Concept to Flight," NASA SP-2000-4517, 2000. https://history.nasa.gov/monograph17.pdf

[23] Kohlman, D. L., *Introduction to V/STOL Airplanes*, Iowa State University Press, Ames, Iowa, 1981.

[24] Flight Optimization System (FLOPS) Software, V.9, NASA, 2020. https://software.nasa.gov/software/LAR-18934-1

[25] SolidWorks 3D CAD, Dassault Systèmes SolidWorks Corporation, 2021. https://www.solidworks.com/product/solidworks-3d-cad

[26] "T700/T6A & T700/T6A1 turboshaft engines," *GE Aviation*, Cincinnati, Ohio, June 2014. https://www.geaviation.com/sites/default/files/datasheet-T700-T6A.pdf

[27] Pike, J., "M-130 General Purpose Dispenser," *FAS Military Analysis Network*, 2000. https://fas.org/man/dod-101/sys/ac/equip/m-130.htm

[28] "AGM-65 Maverick," *U.S. Air Force*, Accessed 2021. https://www.af.mil/About-Us/Fact-Sheets/Display/Article/104577/agm-65-maverick/

[29] "MK-82 500 lb, Free Fall, General Purpose Bomb," *U.S. Air Force*, Accessed 2021. https://www.af.mil/News/Art/igphoto/2000424176/

[30] "LAU-68 F/A Extended Length," *Arnold Defense*, 2021. https://www.arnolddefense.com/product/lau-68-f-a/

[31] Parsch, A., "Air-Launched 2.75-Inch Rockets," *Directory of U.S. Military Rockets and Missiles*, 2006. https://www.designation-systems.net/dusrm/app4/275in-rockets.html

[32] "Star SAFIRE II," *FLIR Systems, Inc.*, 2011. https://www.flir.com/support/products/star-safire-ii/#Documents

[33] "M-197 20 mm Gatling Gun," *General Dynamics*, St. Petersburg, Florida, February 2014. https://www.gd-ots.com/wp-content/uploads/2017/11/M-197.pdf

[34] Lewis, R., "The Art of Strafing," Air Force Magazine, 1 July 2007. https://www.airforcemag.com/article/0707strafing/

[35] Englar, R., and Kirkpatrick, D., "Parametric Trade-off Analysis for Tilting Free Propulsor V/STOL Aircraft in Equilibrium Transition," Naval Ship Research and Development Center, Department of Aerodynamics, 1969. https://apps.dtic.mil/dtic/tr/fulltext/u2/703669.pdf

[36] FlightStream, Version 2020.1, DARcorporation, https://www.darcorp.com/contact-dar-corporation/#tab-7a769cde134eff89e53

[37] Churchill, G. B., "Evaluation of Geared Flap Control System for Tiltwing V/STOL Aircraft," Boeing, Code Ident. No. 77272 D8-207C, Philadelphia, Pennsylvania, Jan 1969. https://apps.dtic.mil/sti/pdfs/AD0712645.pdf

[38] McCormick, B., *Aerodynamics of V/STOL Flight*, Academic Press, Inc., New York, 1967.

[39] Kurzke, J., GasTurb, Version 13, GasTurb GmbH, Aachen, Germany, 2021. https://gasturb.de/download.html

[40] Drela, M., XROTOR, Version 7.55, Massachusetts Institute of Technology, Massachusetts, 2021. https://web.mit.edu/drela/Public/web/xrotor/

[41] Snyder, C. A., and Tong, M. T., Modeling Turboshaft Engines for the Revolutionary Vertical Lift Technology Project, *NASA*, Vertical Flight Society's 75th Annual Forum and Technology Display, Philadelphia, PA, May 2019. https://ntrs.nasa.gov/api/citations/20190025407/downloads/20190025407.pdf

[42] Cavallo, C., "6061 Aluminum vs. 7075 Aluminum - Differences in Properties, Strength and Uses," *Thomas*, 2021. https://www.thomasnet.com/articles/metals-metal-products/6061-aluminum-vs-7075-aluminum

[43] Bai, S., Li, X., Xie, Z., Zhou, Z., and Ou, J., "A Wireless Fatigue Monitoring System Utilizing a Bio-Inspired Tree Ring Data Tracking Technique," *Sensors*, 14(3), 4364–4383, Basel, Switzerland, 2014. https://doi.org/10.3390/s140304364

[44] Sadraey, M., Aircraft Design: A Systems Engineering Approach, Wiley, United Kingdom, 2013.

[45] "Global Aviation Tires," The Goodyear Tire & Rubber Company, Akron, Ohio, 2018. https://www.goodyearaviation.com/resources/pdf/databook-6-2018.pdf

[46] Raymer, D., *Aircraft Design: A Conceptual Approach*, 2nd ed, AIAA, Washington, D.C., 1992.

[47] Roskam, J., *Airplane Design*, Roskam Aviation and Engineering Corporation, Ottawa, Kansas, 1985.

[48] "RF-IR Stealth (Techniques/Benefits)," *Aircraft 101*, 4 March 2016. https://basicsaboutaerodynamicsandavionics.wordpress.com/2016/03/04/stealth-techniques-and-benefits/

[49] Advanced Aircraft Analysis, Version 4.0, DARcorporation, 2021. https://www.darcorp.com/advanced-aircraft-analysis-new-release/

[50] Gouré, D., "The A-29 Super Tucano is the international market leader for light attack aircraft," *Lexington Institute*, 2019. https://www.lexingtoninstitute.org/the-a-29-super-tucano-is-the-international-market-leader-for-light-attack-aircraft/

[51] Hunter, J., "USAF receives first Beechcraft AT-6E Wolverine," *Skies Magazine*, 18 February 2021. https://skiesmag.com/news/usaf-receives-first-beechcraft-at6e-wolverine/

[52] Landay, J., Strobel, W., and Stewart, P., Factbox: The A-29 Super Tucano aircraft at a glance, *Reuters*, 2016. https://www.reuters.com/article/us-usa-nigeria-arms-factbox-idUSKCN0XX09U

[53] DOD, Program Acquisition Cost by Weapon System, *Office of the Under Secretary of Defense (Comptroller)/Chief Financial Officer*, February 2020. https://comptroller.defense.gov/Portals/45/Documents/defbudget/fy2021/fy2021_Weapons.pdf

[54] Everstine, B. W., "How the OA-X Might Change Air Force Acquisition," *Air Force Magazine*, 28 Nov 2017. https://www.airforcemag.com/article/how-the-oa-x-might-change-air-force-acquisition/